Title
Two-Dimensional Graphitic Carbon Nitride (g-C3N4) Nanosheets and Their Derivatives for Diagnosis and Detection Applications

Journal
Journal of Functional Biomaterials, 13(4)

ISSN
2079-4983

Authors
Pourmadadi, Mehrab
Rajabzadeh-Khosroshahi, Maryam
Saeidi Tabar, Fatemeh
et al.

Publication Date
2022

DOI
10.3390/jfb13040204

Journal of *Functional Biomaterials*

MDPI

Review

Two-Dimensional Graphitic Carbon Nitride (g-C_3N_4) Nanosheets and Their Derivatives for Diagnosis and Detection Applications

Mehrab Pourmadadi [1], Maryam Rajabzadeh-Khosroshahi [1], Fatemeh Saeidi Tabar [1], Narges Ajalli [1], Amirmasoud Samadi [1,2], Mahsa Yazdani [1,3], Fatemeh Yazdian [4], Abbas Rahdar [5,*] and Ana M. Díez-Pascual [6,*]

1 School of Chemical Engineering, College of Engineering, University of Tehran, Tehran 14179-35840, Iran
2 Department of Chemical and Biomolecular Engineering, 6000 Interdisciplinary Science & Engineering Building (ISEB), Irvine, CA 92617, USA
3 Department of Biomedical Engineering, State University of New York at Buffalo, Buffalo, NY 14260, USA
4 Department of Life Science Engineering, Faculty of New Science and Technologies, University of Tehran, Tehran 14179-35840, Iran
5 Department of Physics, Faculty of science, University of Zabol, Zabol 538-98615, Iran
6 Universidad de Alcalá, Facultad de Ciencias, Departamento de Química Analítica, Química Física e Ingeniería Química, Ctra. Madrid-Barcelona, Km. 33.6, 28805 Alcalá de Henares, Madrid, Spain
* Correspondence: a.rahdar@uoz.ac.ir (A.R.); am.diez@uah.es (A.M.D.-P.)

Abstract: The early diagnosis of certain fatal diseases is vital for preventing severe consequences and contributes to a more effective treatment. Despite numerous conventional methods to realize this goal, employing nanobiosensors is a novel approach that provides a fast and precise detection. Recently, nanomaterials have been widely applied as biosensors with distinctive features. Graphite phase carbon nitride (g-C_3N_4) is a two-dimensional (2D) carbon-based nanostructure that has received attention in biosensing. Biocompatibility, biodegradability, semiconductivity, high photoluminescence yield, low-cost synthesis, easy production process, antimicrobial activity, and high stability are prominent properties that have rendered g-C_3N_4 a promising candidate to be used in electrochemical, optical, and other kinds of biosensors. This review presents the g-C_3N_4 unique features, synthesis methods, and g-C_3N_4-based nanomaterials. In addition, recent relevant studies on using g-C_3N_4 in biosensors in regard to improving treatment pathways are reviewed.

Keywords: diagnosis; graphitic carbon nitride; biosensors; nanomaterials; antimicrobial activity biomedical applications

Citation: Pourmadadi, M.; Rajabzadeh-Khosroshahi, M.; Saeidi Tabar, F.; Ajalli, N.; Samadi, A.; Yazdani, M.; Yazdian, F.; Rahdar, A.; Díez-Pascual, A.M. Two-Dimensional Graphitic Carbon Nitride (g-C_3N_4) Nanosheets and Their Derivatives for Diagnosis and Detection Applications. *J. Funct. Biomater.* **2022**, *13*, 204. https://doi.org/10.3390/jfb13040204

Academic Editor: John H.T. Luong

Received: 29 September 2022
Accepted: 23 October 2022
Published: 26 October 2022

1. Introduction

The early detection of the biomarkers of the diseases plays a significant role in their treatment and control. It is essential to detect biomarkers associated with a disease early and with the high precision for diagnosis, treatment, and prognosis of fatal diseases, such as cancer, which causes a high mortality rate yearly, and neurodegenerative disorders [1–4]. There are some current conventional diagnostic methods, such as blood tests, imaging, and biopsies, which can be expensive and time-consuming with low sensitivity. Moreover, they require trained personnel, limiting their availability to low-income patients [3].

Today, biosensors are used for detection approaches, such as the high-resolution imaging, fast detection, and monitoring of diseases. Biosensors consist of three main components: recognition, signal transducer, and processor, designed to determine specific biomolecules [5]. These biomolecules can be macromolecules, such as nucleic acid and proteins, or small molecules, such as glucose. Various cancer biomarkers, such as BRCA1, BRCA2, CA 15-3, and CA 125 for breast cancer and PSA for prostate cancer, can be detected as well [6].

Nanotechnology has allowed advances in monitoring, diagnosis, prognosis, and proposing effective treatments [7–16]. In this sense, biosensors based on nanomaterials have accurate detection, efficient monitoring, and fast but reliable imaging [17,18]. The physicochemical properties of nanomaterials, such as photoemission, high specific surface leading to extra bioreceptor immobilization, as well as electrical and heat conductivities, make them perfect candidates for biosensor construction [19–23]. Graphene/graphene oxide, carbon quantum dots, gold nanoparticles, carbon nanotubes, porous carbon, and fullerene are nanostructures that have been investigated as the biosensing platforms studied over the years [24–33]. Carbon nanostructure-based sensors are utilized due to their potential to quench fluorescently-labeled probes [16–21]. Thus, developing a user-friendly and highly sensitive biosensor is essential. Graphitic carbon nitride (g-C_3N_4) nanosheet is another widely used carbon nanostructure to design biosensors [34–39]. g-C_3N_4 nanosheets have high fluorescence quantum yield, superior chemical and thermal stability, are easy to synthesize with low toxicity, and have a low price and high biocompatibility together with unique photoelectrochemical and electroluminescent characteristics [40,41]. Furthermore, the optical properties and conductivity of g-C_3N_4 have made it applicable in optical and electrochemical biosensing approaches. For instance, sulfur-doped graphitic carbon nanosheets (s-g-C_3N_4) as a dual (electrochemical and fluorescence) biosensing platform were used for the detection of cancer biomarkers even at very low concentrations (CA15-3) [42]. This review summarizes the properties and synthesis methods of graphitic carbon nitride nanosheets, which make them highly suitable candidates for the next generation of biosensors.

2. g-C_3N_4-Based Materials: Properties

g-C_3N_4 is a polymeric nanosheet with a graphene-like structure consisting of sp^2 bonded carbon and nitrogen atoms with abundant amino groups on its surface and suitable bandgap energy of 2.7 eV [43]. Thanks to the g-C_3N_4 electronic band structure with sp^2 hybridization, it is considered a photon-harvesting semiconductor material that plays a critical role in detecting biomolecules by photoelectrochemical (PEC) biosensors [44]. Due to the presence of melamine in the π-conjugated nanosheets, g-C_3N_4 is fluorescent with high photoluminescence quantum yield with high and minor absorption at 365 nm and visible light region, respectively [45,46], which can be quenched by materials, such as metal ions, nitrobenzene derivate, or biomolecules, such as heparin and sialic acid, which allow its use as a fluorescent probe biosensor [47] with high photostability and no obvious photobleaching under UV light excitation for 10 h [48]. Furthermore, the g-C_3N_4 ability to convert light and electricity makes it a suitable option for electrochemiluminescence-based and photoelectrochemistry-based biosensing [39]. Various precursors have been proposed for g-C_3N_4 synthesis through thermal condensation. These compounds are rich in nitrogen and contain a tri-s-triazine ring structure, such as dicyandiamide, urea, cyanamide, or thiourea [49]. For instance, if cyanamide is selected as the precursor, thermal heating results in dicyanamide, melamine, melem, and g-C_3N, respectively.

The molecular structures of the g-C_3N_4 precursors and the corresponding temperatures for their thermal condensation are depicted in Figure 1.

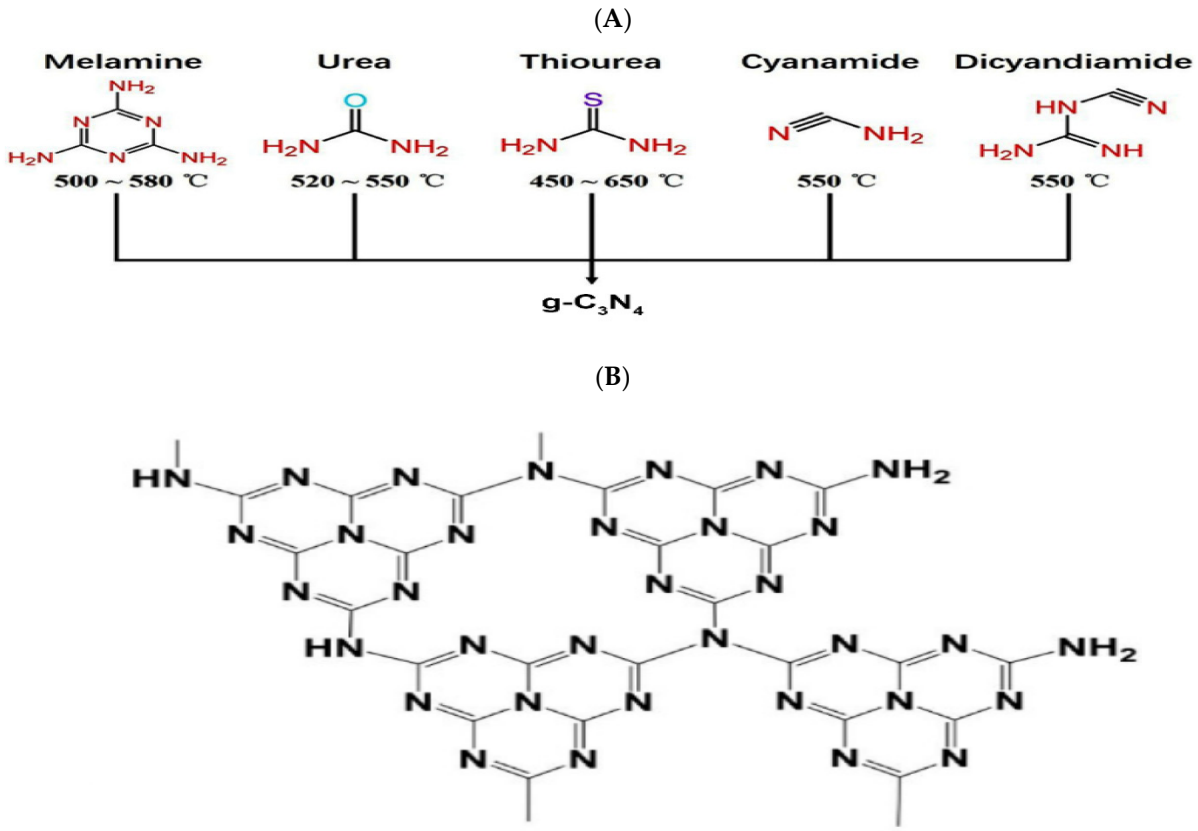

Figure 1. (**A**) Various g-C_3N_4 precursors and the corresponding temperatures for their thermal condensation into g-C_3N_4-, adapted from reference [50] under the terms and conditions of the Creative Commons Attribution (CC BY) license. (**B**) g-C_3N_4 structure, adapted from reference [51] under the terms and conditions of the Creative Commons Attribution (CC BY) license.

In addition, g-C_3N_4 has been reported to display antimicrobial activity. A number of parameters, including the g-C_3N4 band gap, intermediate defect states, dispersed surface area, absorbance in suspension, and charge separation influence its photocatalytic bacterial inactivation [39]. Thus, the modification of this properties influences the production of reactive oxygen species, hence the antibacterial activity. The bactericidal rates of more than 99% have been successfully achieved for eight kinds of foodborne pathogenic bacteria with 8 h incubation in the dark. Cell rupture caused by direct mechanical contact between g-C_3N_4 and cell membranes has been observed. Molecular dynamics simulations further indicated that the presence of large defects in g-C_3N_4 enhanced the electrostatic attraction between inherent pores and lipid heads, resulting in enhanced antibacterial activity.

The thermal and chemical stability of biosensors is crucial for long shelf lives. g-C_3N_4 nanosheets show high thermal stability in the air (up to 600 °C) thanks to the graphitic graphene-like structure with sp^2 bonds between carbon and nitrogen, providing high chemical stability [52]. g-C_3N_4 has low cytotoxicity and good biocompatibility due to its metal-free structure. Moreover, it has a low production cost, a simple synthesis process, a large specific surface area, easy functionalization, and increased penetration coefficient, allowing the efficient immobilization of molecules in the matrix for biosensing [53]. As g-C_3N_4 materials are increasingly used in biomedicine, improving their biocompatibility and biodegradability properties is a necessity. Therefore, modifications are applied to enhance the biocompatibility, biodegradability, and further development of g-C_3N_4 materials. For instance, Kang et al. showed that successfully inserting abundant disulfide bonds into g-C_3N_4 endowed more biodegradability and biocompatibility, boosting its application in biomedical fields [54]. In another study that was recently conducted for glucose detection in diabetic patients, the addition of metal co-catalysts (Fe(III), Cu(II)) to the structure

via adsorption noticeably enhanced the sensitivity compared to the pristine g-C_3N_4 [55]. Thanks to its easy functionalization, g-C_3N_4 can be adapted to various targets with high sensitivity. For instance, a platform based on proton-functionalized ultrathin g-C_3N_4 nanosheets with a positive charge has been developed for heparin (as a biomolecule with a high negative charge) detection in human serum [56].

3. g-C_3N_4-Based Materials: Synthesis Methods

3.1. Synthesis of g-C_3N_4 Nanosheets

The classification of the synthesis methods based on the synthesis procedure can be divided into bottom-up and top-down categories. The "bottom-up" approach generally applies small-sized particles to assemble complex structures. However, the "top-down" procedure is based on splitting large-sized and thick bulks into small particles and thin nanosheets [57,58]. The bottom-up procedure includes ionic liquid, supramolecular pre-assembly, and hydrothermal methods [58]. In the bottom-up approach, g-C_3N_4 sheets are synthesized on a large scale via thermal polymerization (pyrolysis) or the carbonization of small organic compounds (that contain hydroxyl, carboxyl, carbonyl, and primary amine functional groups) [59], such as melamine, cyanimide, Dicyanamide, or urea [60]. Dante et al. obtained g-C_3N_4 from the pyrolysis of melamine cyanurate at 650 °C for 50 min (in the crucible with atmosphere condition), which was used for glucose sensing [55]. On the other hand, chemical exfoliation and ultrasonic exfoliation methods have been utilized for the top-down approach. Chemical exfoliation is more common for large-scale production due to its high efficiency and the easier tuning of the g-C_3N_4 structure [61]. For example, Hatamie et al. used g-C_3N_4 as a label-free fluoro-sensor to analyze the amount of metronidazole in biological fluids and drug samples. g-C_3N_4 ultrathin nanosheets were synthesized in bulk via the thermal polymerization method from melamine, possessing a highly π-conjugated structure at 600 °C. The exfoliation procedure was performed through ultrasonication in water media [62].

3.2. Synthesis of g-C_3N_4-Based Composites

g-C_3N_4 properties can be enhanced through its fabrication with other materials into composites. In the modification techniques, metal loading is critical for increasing the potential application of g-C_3N_4 biosensors due to outstanding electrochemical qualities. Metal/g-C_3N_4 composites are produced with solvothermal treatment, photo-deposition, precipitation, and thermal polymerization methods [63]. Generally, there are numerous ways to prepare g-C_3N_4-based nanocomposites. The simple pyrolysis method, solution (sonication) mixing, the hydrothermal method, the simple calcination method, the hydrolysis method, sol-gel, and microwave irradiation are some synthesis methods that have been applied in the formation of nanocomposites based on g-C_3N_4- and have been utilized for different applications [43]. The pyrolysis method is a common way to produce g-C_3N_4-based composites in diagnosis applications where the mixture of the precursor of g-C_3N_4 and the other components is calcinated in a crucible for a while with a specific heating rate and initial temperature to prepare the nanocomposite. Then, the product is cooled at 25 °C. For example, a sensitive electrochemical sensor for dopamine detection was fabricated by firstly preparing calcium stannate ($CaSnO_3$) nanoparticles from $CaCl_2$ and $SnCl_2.2H_2O$ via the hydrothermal method, then $CaSnO_3$-gC_3N_4 nanohybrid was produced through the pyrolysis of melamine, $(NH_4)_2SO_4$, and $CaSnO_3$ mixture at 550 °C in a crucible [64]. In another study for glucose detection, Cu(II)–Fe(III)-g-C_3N_4 was prepared through the sonication method (2 h sonication of a suspension of 416 mg of g-C_3N_4 in a 20 mL aqueous solution containing Cu(II) and Fe(III) ions), which led to the adsorption of ions on the g-C_3N_4 structure [55]. A highly selective glucose-sensing (in human blood) biosensor based on ultrathin g-C_3N_4 nanosheets doped with niobium (Nb) metal was synthesized by the pyrolysis method from urea [65]. A biosensor for 4-nitrophenol detection was developed by Vinoth et al. 4-nitrophenol is a very poisonous chemical compound released into the water during the production of some drugs, dyes, and leather, posing human health at high risk.

So, for 4-nitrophenol monitoring, the biosensor based on $BaSnO_3$-g-C_3N_4 nanostructure was synthesized by sonication method from prepared $BaSnO_3$ and g-C_3N_4 [66].

4. g-C_3N_4-Based Biosensors

4.1. g-C_3N_4-Based Surface Plasmon Resonance (SPR) Biosensors

Surface plasmon resonance (SPR) sensing is a powerful probe of the interplays between protein–ligand, protein–DNA, protein–protein, and protein–membrane binding [67]. SPR biosensors are a very effective tool for measuring many biomarkers [68]. The main advantages of these biosensors are their fast response and ability to detect various analytes concurrently [69]. Moreover, among various new techniques available, SPR biosensors are the best optical biosensors for label-free, fast, and in situ diagnosis of molecules [40]. SPR is a physical optics phenomenon that can detect biomarkers because of the high sensitivity of surface plasmons to the dielectric medium [70]. In these biosensors, receptors are immobilized on the metal surface, interacting with the analytes and leading to dielectric alteration. This phenomenon affects the resonance condition of surface plasmons with specific surface plasmon waves (SPWs), allowing the transmission of photon's energy to the surface plasmons at the resonance angle resulting in the decrease of the light reflectance and thus the SPR curve [71]. Based on the characteristic of light, the SPR biosensors can be categorized into angular, wavelength, or intensity-modulated systems [72–74]. The Kretschmann configuration is the most recent version of SPR based on attenuated total reflection [54]. At an angle, part of light energy is transmitted to the surface plasmon, and the reflectance can be shown in the angular scanning.

The presence of adsorbed molecules on the biosensor surface varies the refractive index, and the SPR angle is changed accordingly [75].

Two-dimensional (2D) materials with large surface areas, such as g-C_3N_4, can act as the sensitive layers for SPR [40]. Duan et al. designed a surface plasmon resonance (SPR) biosensor based on a 2D nanocomposite of g-C_3N_4 nanosheets and molybdenum disulfide quantum dots (MoS_2QDs), adorned with chitosan-stabilized Au nanoparticles (CS-AuNPs) to detect prostate specific antigen (PSA) selectively. In this work, the MoS_2QDs easily aggregated and reduced the sensitivity, but as a support for MoS_2QDs, the g-C_3N_4 nanosheets improved the biosensing performance for PSA detection. Additionally, the MoS_2QDs@ g-C_3N_4@ CS-AuNPs-based SPR aptasensor showed a very low limit of detection (LOD), 0.77 ng·mL^{-1}, with good linearity range at PSA concentrations in the range of 1.0–250 ng·mL^{-1} [40].

4.2. g-C_3N_4-Based Electrochemical Biosensors

Electrochemical biosensors have been recognized as powerful diagnostic tests over the past years thanks to their unique advantages, such as simplicity, high sensitivity, and accuracy [76]. Three vital components are necessary to develop electrochemical biosensors: (I) a bioreceptor to link with analyte, (II) an electrode, and (III) a read-out system [77]. An electrochemical sensor requires a working reference and an auxiliary electrode; the working electrode in the electrochemical biosensor acts as a transducer in the reaction between the bioreceptor and the analyte. It generates a biological signal which changes into an electronic signal and is processed with high sensitivity [78]. On the other hand, Ag/AgCl-based reference electrode is kept at the site of the reaction to maintain a particular potential. The auxiliary electrode links the electrolytic solution and must be conductive; thus, gold or platinum are suitable candidates [79]. Some electrochemical methods for marker detection include voltammetric techniques (cyclic, square wave, or stripping), impedimetric, and amperometry. Of these techniques, cyclic voltammetry (CV) is preferred [77].

In an electrochemical biosensor, an electrode is the main component for immobilizing electron motion and biomolecules [80]. Nanomaterials have piqued attention due to their unique electronic characteristics [81]. The carbon allotropes can be applied as electrodes due to their effective electron transfer rate and high active surface area. Additionally, carbon nanostructured materials are significant in research due to their unparalleled properties,

such as chemical stability and good conductivity [82]. g-C_3N_4 is a polymeric semiconductor with a specific structure and high stability, making it a good nanocomposite for electrochemical biosensors [83]. g-C_3N_4 is known as the most thermal stable allotrope of carbon nitrides [84], which can be used in the diagnosis system based on its catalytic ability [85]. Due to the low electron conductivity of g-C_3N_4, it has been used with other materials to enhance its surface conductivity. The g-C_3N_4 derivatives can electrically connect to the redox center of biomolecules on the surface of the electrode. The electronic integration of the g-C_3N_4 with various carbon types notably increases the surface area and conductivity [85]. The chemical exfoliation of bulk g-C_3N_4 has been used to develop g-C_3N_4 nanosheets for the detection of neurotransmitters, such as dopamine (DA). Kathiresan et al. developed a glassy carbon electrode (GCE) doped with bulk g-C_3N_4. The electrochemical activation of bulk g-C_3N_4 was performed with a potential of 1.75 V in neutral pH conditions (pH 7.0). In the electrode oxidation reaction, the two-electron process is followed by the transfer of two protons, resulting in 5-HTquinoneimine. Figure 2 illustrates the redox reaction. Oxidation leads to the transfer of protons to form 5-HTquinoneimine and the reduction occurs in the quinone group on 5-HT quinoneimine [86].

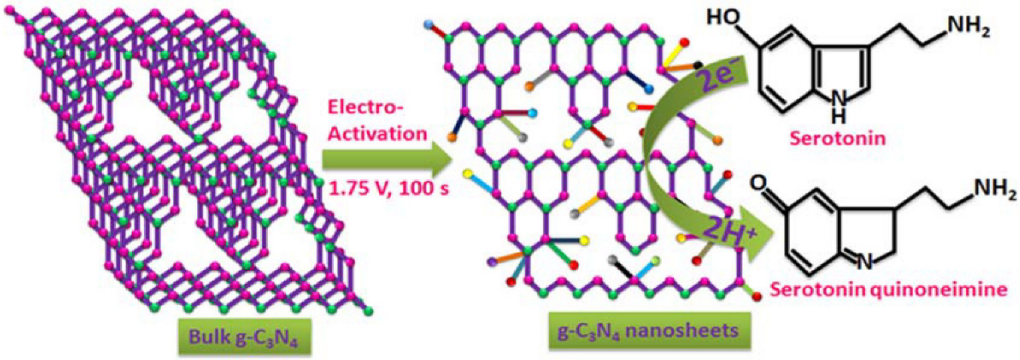

Figure 2. Activation of g-C_3N_4 on glassy carbon electrode and the redox reaction on the developed electrochemical biosensor for serotonin (5-HT)-. Adapted from reference [86] under the terms and conditions of the Creative Commons Attribution (CC BY) license.

Table 1 collects studies conducted on detecting various biomarkers using electrochemical biosensors.

Table 1. Comparison of different biomarkers detection using electrochemical techniques.

Method	Interface	Biomarker	LOD	Dynamic Range	Ref.
Electrochemistry	IL-CNNS	2,4-Dichlorophenol	0.0062 µM	0.02–160 µM	[87]
Electrochemistry	Cu-Al_2O_3-g-C_3N_4-Pd	amyloid β-protein	3.3 fg/mL	10 fg/mL–100 ng/mL	[88]
Electrochemistry	CeO_2/g-C_3N_4	anti-depressant drug Agomelatine (AG)	0.96 ng/mL	1–20 ng/mL	[89]
Electrochemistry	PEDOT/h-CN	ascorbic acid (AA) acetaminophen (AP)	1.51 µM 0.49 µM	4–20, 20–1800 µM 1–10, 10–50 µM	[90]
Electrochemistry	MoS_2QDs@g-C_3N_4@CS-AuNPs	PSA	0.71 pg/mL	-	[40]
Electrochemistry	mpg-C_3N_4	Avian Leukosis Viruses	120 $TCID_{50}$/mL	-	[91]
Electrochemistry	MIP/g-C_3N_4/FTO	bisphenol A	23 µmol L^{-1}	5–200 µmol L^{-1}	[92]
Electrochemistry	Ag/g-C_3N_4	CA 19-9	1.2 mU mL^{-1}	5.0 mU mL^{-1}–50 U mL^{-1}	[93]

Table 1. *Cont.*

Method	Interface	Biomarker	LOD	Dynamic Range	Ref.
Electrochemistry	Au/ g-C_3N_4	chronic lymphocytic leukemia	20 pM	0.6 nM–6.4 nM	[94]
Electrochemistry	Au/mpg-C_3N_4	Cr(VI)	14 ppb	100–1000 ppb	[95]
Electrochemistry	g-C_3N_4/GO	pesticide	8.3 nM	0.045–213 µM	[96]
Electrochemistry	g-C_3N_4-E-PEDOT	acetaminophen	0.034 µM	0.01–2.0, 2.0–100 µM	[97]
diasadiElectrochemistry	C-g-C_3N_4	diphenylamine	0.009 µM	0.008–682 µM	[98]
Electrochemistry	g-C_3N_4/CuO	dopamine	1×10^{-10} mol L^{-1}	2×10^{-9}–7.11×10^{-5} mol L^{-1}	[99]
Electrochemistry	Ru^0 /PANI@g-C_3N_4	Bisphenol-A	0.18 nM	0.01–1.1 µM	[100]
Electrochemistry	Co_3O_4/g-C_3N_4	environmental phenolic hormones	3.3×10^{-9} mol L^{-1}	1.0×10^{-8}–1.2×10^{-5} mol L^{-1}	[101]
Electrochemistry	V_2O_5/g-C_3N_4/PVA	folic acid	0.0017 µM	0.01–60 µM	[102]
Electrochemistry	VC/g-CN NSs	Furazolidone	0.5 nM	0.004−141 µM	[103]
Electrochemistry	g-C_3N_4/MoO_3	Furazolidone	1.4 nM	0.01–228 µM	[104]
Electrochemistry	g-C_3N_4@Au NPs	galectin-3	25.0 fg mL^{-1}	0.0001–20.0 ng mL^{-1}	[105]
Electrochemistry	Pt^{2+}@g-C_3N_4	glucose	10 µM	13–2000 µM	[106]
Electrochemistry	g-C_3N_4	glucose	5 µM	50 µM–2 mM	[107]
Electrochemistry	g-C_3N_4/Fe_2O_3-Cu	glucose	0.3 µM	0.6 µM-2.0 mM	[108]
Electrochemistry	g-C_3N_4−CH	Hg(II)	0.010 µmol L^{-1}	1.00−80.0, µmol L^{-1} 0.100−5.00 µmol L^{-1}	[109]
Electrochemistry	g-C_3N_4 and Hg(II)-imprinted polymer	Hg(II)	0.018 nmol L^{-1}	0.06–25 nmol L^{-1}	[110]
Electrochemistry	Pt /g-C_3N_4/ Polythiophene	Hg^{2+}	0.009 nM	1–500 nM	[111]
Electrochemistry	Utg-C_3N_4	Hg(II)	0.023 µg/L	0.1–15.0 µg/L	[112]
Electrochemistry	g-C_3N_4-F127-Au NSs	HSP90	2.67 µg/mL	3.5 µg/mL–2.43 mg/mL	[113]
Electrochemistry	Co_3O_4/g-C_3N_4	hydrazine	1 µM	5–1000 µM	[114]
Electrochemistry	S-g-C_3N_4/FTO	hydrazine	0.06 µM	60 µM–475 µM	[115]
Electrochemistry	PANI/g-C_3N_4/AgNPs	hydrazine	300 µM	5–300 mM	[116]
Electrochemistry	Cu/MnO_2/g-C_3N_4	hydrogen peroxide	0.85 µM	10–20,000, 20,000–400,000 µM	[117]
Electrochemistry	Na,O-g-C_3N_4	hydrogen peroxide	0.05 µM	1 µM–50 µM	[118]
Electrochemistry	g-C_3N_4/HOPG	hydrogen peroxide	0.12 µM	0.12–120 µM	[119]
Electrochemistry	rGO/g-C_3N_4	Pb(II)	1.07×10^{-12} mol/L	-	[120]
Electrochemistry	$CsTi_2NbO_7$@g-C_3N_4	nitrite	2.63×10^{-5} mol/L	0.0999–3.15 mmol/L	[121]
Electrochemistry	ZSO-gCN	nitrobenzene	2.2 µM	30–100 µM	[122]
Electrochemistry	Ox-g-C_3N_4	Norovirus-Specific DNA	100 fM	-	[123]

Table 1. *Cont.*

Method	Interface	Biomarker	LOD	Dynamic Range	Ref.
Electrochemistry	g-CNNS	ochratoxin A	0.073 nM	-	[124]
Electrochemistry	AChE/CS/Pd WLNCs/g-C_3N_4	acetylthiocholine (ATCl)	0.67 nM	0.002–2.46 µM	[125]
Electrochemistry	g-C_3N_4	oxalic acid	0.75×10^{-6} mol L^{-1}	$(1–1000) \times 10^{-6}$ mol L^{-1}	[126]
Electrochemistry	g-C_3N_4/PEDOT-MeSH	paracetamol	1 µM	0.4–1280 µM	[127]
Electrochemistry	g-C_3N_4 /CuO	p-nonylphenol	1.2×10^{-8} mol·L^{-1}	3.0×10^{-8}–5.1×10^{-6} mol·L^{-1}	[128]
Electrochemistry	HP5@AuNPs@g-C_3N_4	PSA	0.12 pg mL^{-1}	0.0005–10.00 ng mL^{-1}	[129]
Electrochemistry	AuNP/g-C_3N_4	PSA	5.2 pg mL^{-1}	0.01–30 ng mL^{-1}	[130]
Electrochemistry	g-C_3N_4/NiO	quercetin	0.002 µM	0.010–230 µM	[131]
Electrochemistry	Pt/g-C_3N_4/Polyaniline	Hg^{2+}	0.014 nM	1–500 nM	[132]
Electrochemistry	Bi_2Te_3@g-C_3N_4 BNs	ractopamine (RAC)	1.77 nM	0.015–456.4 µM	[133]
Electrochemistry	AuOct-PEI-C_3N_4	sulfamethazine	6.9×10^{-5} ng·mL^{-1}	0.0001–100 ng·mL^{-1}	[134]

4.3. g-C_3N_4-Based Photoelectrochemical (PEC) Biosensors

The photoelectrochemical (PEC) detection method is a hopeful technique for biological assays [135], which is also a low-cost approach to transforming chemical energy into electricity under a flash of light [136], and PEC biosensors have become prominent due to their capability of biomolecules diagnosis. This method has had much consideration because of its high sensitivity, simplicity, and fast response [137]. In the PEC diagnosis system, light is used as an excitation source [138], allowing for a high sensitivity with low background signals [136]. The PEC cell includes three main components: (a) a light-harvesting semiconductor, (b) a metal electrocatalyst, and (c) adequate electrolytes among the working electrode and auxiliary electrode to generate PEC signals using redox reaction. Upon illumination, the redox reactions lead to a signal between the working and the auxiliary electrodes [139].

PEC biosensors use wide bandgap semiconductors as photoactive materials [63], changing optical energy to electrical and chemical energy [140]. g-C_3N_4 is a responsive photocatalyst with a bandgap (2.7 eV) [141]. Additionally, one of the promising approaches is a photocatalytic reaction which can absorb visible light [82]. g-C_3N_4, as an inorganic polymeric semiconductor, possesses a graphite-like layer structure [142]. So, PEC biosensors show advantages over electrochemical and optical biosensors with high sensitivity and low cost. Hence research in the PEC biosensor for analyte detection has increased. Biomarkers detected using photoelectrochemical biosensors are summarized in Table 2.

Table 2. Using photoelectrochemical (PEC) techniques for biomarkers detection.

Method	Interface	Biomarker	LOD	Dynamic Range	Ref.
PEC	ZnO@CdTe nanocable arrays/carboxylated g-C_3N_4	Proprotein convertase subtilisin/kexin type 6 (PCSK6)	2 pg/mL	10 pg/mL–20.0 ng/mL	[143]
PEC	ZnO/MoS_2/g-C_3N_4	5-hydroxymethylcytosine (5hmC)	2.6 pM	0.01–200 nM	[144]

Table 2. *Cont.*

Method	Interface	Biomarker	LOD	Dynamic Range	Ref.
PEC	CuO-g-C_3N_4	aflatoxin B1	6.8 pg mL^{-1}	0.01 ng mL^{-1}–1 µg mL^{-1}	[145]
PEC	TiO_2/g-C_3N_4	alkaline phosphatase	0.03 U/L	-	[146]
PEC	g-C_3N_4	chloramphenicol	0.22 pM	1 pM–100 nM	[147]
PEC	g-C_3N_4/TiO_2	ascorbic acid alkaline phosphatase	0.3 nM 0.1 mU/L	1 nM–10 µM 0.3 mU/L–1 U/L	[148]
PEC	AuNPs/g-C_3N_4	avian viruses	85 $TCID_{50}$/mL	-	[149]
PEC	$Zn_{0.1}Cd_{0.9}S$/g-C_3N_4	Carcinoembryonic Antigen	1.4 pg·mL^{-1}	0.005 ng·mL^{-1}–20 ng·mL^{-1}	[150]
PEC	g-C_3N_4/$CuInS_2$	Carcinoembryonic Antigen	5.2 pg mL^{-1}	0.02−40 ng mL^{-1}	[151]
PEC	g-C_3N_4/CdSe	Carcinoembryonic Antigen	0.21 ng mL^{-1}	10 ng mL^{-1}–100 µg mL^{-1}	[152]
PEC	ZnO NDs@g-C_3N_4 QDs	CCRF-CEM cell	20 cell/mL	20–20,000 cell/mL	[153]
PEC	Ag_2CrO_4/g-C_3N_4/GO	chloramphenicol	0.29 pM	0.5 pM–50 nM	[154]
PEC	P-g-C_3N_4-WS_2	5- formylcytosine	3.8 pM	0.01–200 nM	[155]
PEC	g-C_3N_4/Ti_3C_2	ciprofloxacin	0.13 nM	0.4–1000 nM	[156]
PEC	Cu-BTC MOF/g-C_3N_4	glyphosate	1.3×10^{-13} mol L^{-1}	1.0×10^{-12}–1.0×10^{-8} mol L^{-1} and 1.0×10^{-8}–1.0×10^{-3} mol L^{-1}	[157]
PEC	g-C_3N_4@CdS QDs	Hg^{2+}	12 nM	20–550 nM	[158]
PEC	TiO_2/g-C_3N_4/ graphene	dopamine	0.02 µM	0.1 to 50 µM	[159]
PEC	GOx|g-C_3N_4-TiO_2|ITO	glucose oxidase	0.01 mM	0.05–16 mM	[160]
PEC	GOx-β-Gal@Au NPs-g-C_3N_4-MnO_2-TiO_2/ITO	Glucose and Lactose	0.23 mM	0.008–2.50 mM	[161]
PEC	g-C_3N_4/$ZnIn_2S_4$	glucose	0.28 µM	1–10,000 µM	[162]
PEC	utg-C_3N_4/WO_3/ITO	glucose	0.0001 mM	0.01–7.12 mM	[163]
PEC	$Mn_3(BTC)_2$/g-C_3N_4/TiO_2	H_2O_2	0.001 µM	0.003–10 µM	[164]
PEC	g-C_3N_4/P3HT	H_2O_2	0.38 µM	1.0–800 µM	[165]
PEC	g-C_3N_4/CdS quantum dots	methylated RNA	3.53 pM	0.01-10 nM	[166]
PEC	g-C_3N_4/CdS quantum dots	DNA MTase	0.316 U/mL	1–80 U/mL	[167]
PEC	cg-C_3N_4	Metronidazole	0.005 µM	0.01–100 µM	[168]
PEC	Au/CeO_2/g-C_3N_4	Microcystin-LR	0.01 pM	0.05–10^5 pM	[169]
PEC	MoS_2/g-C_3N_4/black TiO_2	microRNA	0.13 fM	0.5 fM–5000 fM	[170]
PEC	CdS@g-C_3N_4	MicroRNA	0.05 fM	0.1 fM–1.0 nM	[171]
PEC	g-C_3N_4-MoS_2@CdS:Mn	myoglobin	0.42 pg mL^{-1}	1.0 pg mL^{-1}–50 ng mL^{-1}	[172]
PEC	PPy/g-C_3N_4/WO_3 IOPCs	Oxytetracycline (OTC(	0.004 nM	0.01–5 nM	[173]
PEC	g-C_3N_4/WO_3 IOPCs	Oxytetracycline (OTC(	0.12 nM	1 nM–230 nM	[174]

For instance, Li et al. developed a PEC biosensor based on coral-like g-C_3N_4 nanostructures to detect the metronidazole biomarker. Although metronidazole is a common antibacterial drug, it causes carcinogenic and genotoxic issues. Hence, the sensitive and facile detection of metronidazole's residues in typical oral medicine samples is an effective

approach in health care. According to the results, coral-like g-C_3N_4 nanostructures in the biosensor platform boosted the facility of signal amplification in the PEC sensing [168]. In the other study, Mao et al. applied the photosensitive CuO-g-C_3N_4 nanostructures as an efficient photocathode in the PEC sensing of aflatoxin B1 (as a food contaminator and class 1 carcinogen). The conjugation of CuO to g-C_3N_4 efficiently extended the optical absorption toward the visible region. The CuO-g-C_3N_4 nanocomposite enhanced the PEC signaling for the sensitive detection of aflatoxin B1 [145].

4.4. g-C_3N_4-Based Fluorescent Biosensors

Fluorescent biosensors have been used in biological assays, owing to their high sensitivity, simple readout systems, lower response time, and visualization [175]. Fluorescent biosensors possess a specific ability to monitor biological cell targets [176,177]. Fluorescence spectroscopy has been widely applied to determine cancer and heavy metal ions [178,179]. Accordingly, the important advantages of this type of biosensor are that it is non-invasive, its capability to use fluorescence intensity, and its fluorescence lifetime. Additionally, using fluorescent nanomaterials, biomarker diagnosis can be highly selective and sensitive [180]. Fluorescent biosensors function by absorbing electromagnetic radiation, which is absorbed by fluorophores or fluorescently labeled molecules. Fluorescent biosensors can be divided into four types according to the signal-producing technique, including FRET (Forster Resonance Energy Transfer), FLIM (Fluorescence Lifetime Imaging), FI (Fluorescence Intensity and its change), and FCS (Fluorescence Correlation Spectroscopy) [181]. The fluorescence biosensors have a single signal for detection and can easily be disturbed by environmental and instrumental conditions [182]. In luminescence, light is produced by excitation without increasing the temperature. Fluorescence is a type of luminescence that occurs over a short period and is created by electromagnetic excitation [183]. Moreover, in fluorescence, the time interval between absorption and emission is short [184]. Figure 3 shows the various schemes of fluorescent reagent-less protein-based biosensors [185].

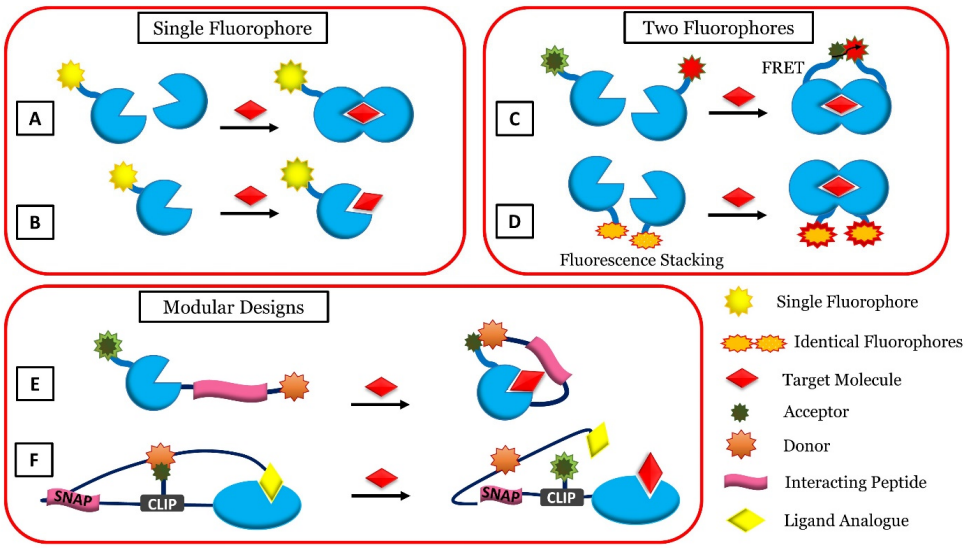

Figure 3. Different schemes of fluorescent reagent-less protein-based biosensors. Single-fluorophore-based biosensors: Change in conformation (**A**) or target interaction (**B**) changes the environment of fluorophore. Two-fluorophore-based biosensors: In between two different fluorophores, FRET is recorded (fluorescent proteins) (**C**), or by breaking the stack of two fluorescent dyes which are identical (**D**). Modular design-based biosensors: a part in the merged system with the recognition element can interact with either the target bound (**E**) or the target-free state (**F**) so that when the target binds, the signal is transduced, Reproduced from Ref. [185] under the terms and conditions of the Creative Commons Attribution (CC BY) license.

Nanomaterials have introduced an attractive method of developing low-cost and portable fluorescent devices [186]. In recent decades, a new group of 2D nanomaterials has attracted research attention. g-C_3N_4 nanosheets supply an iterating choice for bioimaging and bioprobes applications [187,188]. Additionally, the N-contain structure for the g-C_3N_4 nanosheet provides the potency for coordination with proton or metal ions [189]. The mentioned unique characteristics of g-C_3N_4 nanosheets make this useful for developing fluorescent biosensors or bioprobes. Table 3 shows some of the developed fluorescent biosensors for detecting different biomarkers.

Table 3. Fluorescent techniques developed for various biomarkers.

Method	Interface	Biomarker	LOD	Dynamic Range	Ref.
Fluorescent	S-Doped g-C_3N_4 Pinhole Porous Nanosheets	Ag^+	57 nM	0 to 1000 nM	[190]
Fluorescent	g-C_3N_4	ascorbic acid	5.3nM	0–26.67 nM	[191]
Fluorescent	mpg-C_3N_4	Au^{3+}	1.1 µM	-	[192]
Fluorescent	g-C_3N_4	chromium (VI)	0.15 µM	0.6 µM–300 µM	[193]
Fluorescent	g-C_3N_4	CN^- $Cr_2O_7{}^{2-}$	1.5 µM 18 nM	- -	[194]
Fluorescent	g-C_3N_4	copper(II)	8 pM	0.01–0.4 nM	[195]
Fluorescent	g-C_3N_4	cytochrome C	2.6 nM	16–140 nM	[196]
Fluorescent	g-C_3N_4	Ag^+ S^{2-}	4.2 nM 3.5 nM	0–40 nmol /L 0–30 nmol/L	[197]
Fluorescent	g-C_3N_4 nanosheets/chromogenic	glutathione	0.01 µM	0.05 M L^{-1}–1.0 M L^{-1}	[198]
Fluorescent	g-C_3N_4	dopamine	0.017 µM	0–20 µM	[199]
Fluorescent	WS-g-C_3N_4@AuNCs	Fe^{2+} Cu^{2+}	1.73 nmol L^{-1} 3.63 nmol L^{-1}	-	[200]
Fluorescent	Fe-g-CNO	Fluoride Ions	1×10^{-6} M	-	[201]
Fluorescent	g-C_3N_4@CuMOFs	glucose	59 nM	0.1–22 µM	[202]
Fluorescent	g-C_3N_4−MnO_2	Glutathione	0.2 µM	-	[203]
Fluorescent	g-C_3N_4	Hemin	0.15 µM	0.5–25 µM	[204]
Fluorescent	g-C_3N_4	H_2O_2	0.07 µM	0.1–100 µM	[205]
Fluorescent	g-C_3N_4–Dopa	laccase activity	2 U L^{-1}	0–430 U L^{-1}	[206]
Fluorescent	g-C_3N_4	metronidazole	0.008 µg ml^{-1}	0.01–0.10 µg ml^{-1}	[62]
Fluorescent	Fe_3O_4/g-C_3N_4/HKUST-1	ochratoxin A	2.57 ng/mL	5.0–160.0 ng/mL	[207]

Hatamie et al. applied g-C_3N_4 nanosheets to develop a label-free bioassay system for diagnosing metronidazole in biological fluids. The switch-off green fluorescence biosensor provided rapid sensing with a linear detection range from 0.01 to 0.10 µg mL^{-1} [62]. Dopamine is a neurotransmitter with substantial biological functions in neuroendocrine regulations, and its abnormal content in the human serum leads to Parkinson's and Alzheimer's disease. Lv et al. investigated the g-C_3N_4 nanofibers in the fluorescent probe for dopamine sensing. It provided a sensitive detection platform with a limit of detection (LOD) lower than 17 nM [199].

4.5. g-C_3N_4-Based Electrochemiluminescent (ECL) Biosensors

Over the past several decades, many studies on electrochemiluminescence (ECL) biosensors have been conducted in various fields, such as chemical analysis and clinical diagnostics or food analysis. Electrochemiluminescence, or electrochemical chemiluminescence, is the light emission produced from molecular types by an electron transfer process. Additionally, ECL is triggered by an electrochemical reaction of the luminophores on an electrode surface. Moreover, the significant advantages of ECL are its high sensitivity and selectivity. In ECL biosensors, electrochemically generated intermediates endure an extremely exergonic reaction to turn out into an electronically excited state. ECL-based biosensors utilize specific biological diagnosis elements, such as enzymes, antibodies, aptamers, peptides, and proteins to selectively recognize a particular analyte and generate an ECL signal [208]. The basis of the method is on diagnosis interaction among biological cognizance elements and the corresponding targets by ECL release alterations. Accordingly, two main components are needed in standard ECL detection: ECL active types and biological cognizance elements.

Depending on the reaction that induces the ECL signal emission, there are several sensing systems for medical applications.

In systems that are based on the chemical reactions of the luminophores and co-reactants, the chemical reaction between the luminophore and the co-reactant and is used for detecting diverse biomarkers.

The second type is systems that involve the co-reaction accelerator-involved reactions. In these systems, the reaction mixture is mixed with co-reaction accelerators. These accelerators are involved in generating electrochemiluminescent reactions in terms of facilitating the ECL reaction rate of co-reactant to produce several intermediates.

In systems that incorporate resonance energy transfer (RET) reactions, instead of using only one luminophore, the signal is emitted via two different emitters by incorporating a RET.

For systems that incorporate an enzyme reaction-based signal amplification, binding events between target analytes and probe DNAs initiate. High sensitivity and extension of the dynamic range of the modulation are some of the benefits of these systems [209]. Figure 4 represents the metioned types of ECL biosensors based on the reactions leading to ECL signal emission.

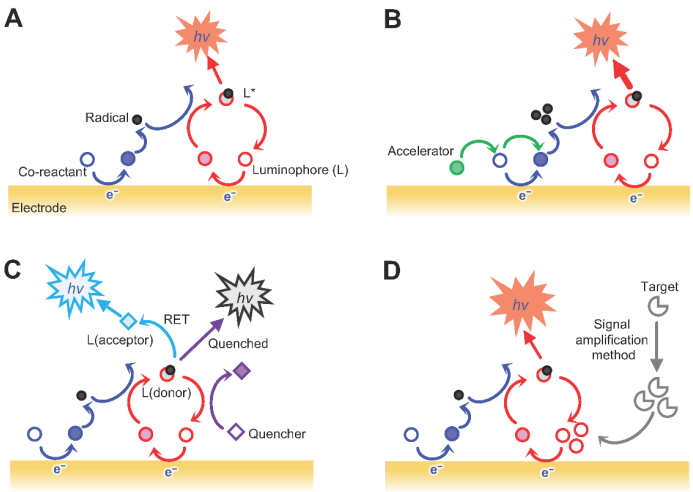

Figure 4. Differet categories of ECL systems. (**A**) Luminophore and co-reactant-involved reaction-based system; (**B**) co-reaction accelerator-involved reaction-mediated system; (**C**) resonance energy transfer (RET) reactions-incorporated system; and a (**D**) signal amplification method-incorporated system. Adapted from Ref. [209] under the terms and conditions of the Creative Commons Attribution (CC BY) license.

g-C_3N_4 has a large surface area, and this carbon-based material can enable more sites to sequester charge carriers. Additionally, g-C_3N_4 has high electron conductivity, and they can successfully separate and then transfer charge carriers [208]. Some of the electrochemiluminescent biosensors are represented in Table 4.

Table 4. (ECL) methods for different biomarkers.

Method	Interface	Biomarker	LOD	Dynamic Range	Ref.
ECL	Au-g-C_3N_4 NHs	alpha fetoprotein	0.0005 ng mL^{-1}	0.001–5 ng mL^{-1}	[210]
ECL	g-C_3N_4	amyloid β peptides	3.25 fM	10 fM–0.1 μM	[211]
ECL	g-C_3N_4@Au NPs coated Pd NPs@NH_2-MIL-53	amyloid β peptides	3.4 fg·mL^{-1}	10 fg·mL^{-1}–50 ng·mL^{-1}	[212]
ECL	Fe_3O_4@g-C_3N_4	CA125	0.4 mU·mL^{-1}	0.001–5 U·mL^{-1}	[213]
ECL	Ag-doped g-C_3N_4	concanavalin A	0.0003 ng·mL^{-1}	0.001–50 ng·mL^{-1}	[214]
ECL	g-C_3N_4	tyramine	1.79 nmol L^{-1}	1×10^{-8} –1×10^{-3} mol L^{-1}	[215]
ECL	C-g-C_3N_4/CuO	dopamine	8.2 nM	10 nM–1 mM	[216]
ECL	g-C_3N_4 NSs–PTCA	dopamine	2.4 pM	6.0 pM–30.0 nM	[217]
ECL	AuNF@g-C_3N_4–PAN	dopamine	1.7×10^{-9} M	5.0×10^{-9}–1.6×10^{-6} M	[218]
ECL	g-C_3N_4 NSs-rGO/$S_2O_8^{2-}$	folic acid	62 pM	0.1–90 nM	[219]
ECL	ZnO@g-C_3N_4	fipronil	1.5 nmol L^{-1}	5–1000 nmol L^{-1}	[220]
ECL	Au-g-C_3N_4	Nuclear factor-kappa B	5.8 pM	-	[221]
ECL	g-C_3N_4 nanosheets and Ag-PAMAM-luminol	HL-60 cancer cells	150 cells	200–9000 cells·mL^{-1}	[222]
ECL	C- g-C_3N_4	insulin	33 fg·mL^{-1}	0.1 pg·mL^{-1}–20.0 ng·mL^{-1}	[223]
ECL	C_{60}/g-C_3N_4 NS	melamine	1.3×10^{-13} M	2.7×10^{-11}–1.9×10^{-8} M	[188]
ECL	g-C_3N_4/$K_2S_2O_8$	methotrexate (MTX)	0.27 pM	1 pM–10 μM	[224]
ECL	g-C_3N_4@AuNPs	miRNAs	0.3 fM	1 fM–10 pM	[225]
ECL	Ce-MOF@g-C_3N_4/Au	N-terminal pro-B-type natriuretic peptide	3.59 pg mL^{-1}	0.005–20 ng mL^{-1}	[226]
ECL	g-C_3N_4 NSs	Pyrophosphate Ion	75 pM	2.0–800 nM	[227]
ECL	AuNPs/g-C_3N_4	squamous cell carcinoma antigen (SCCA)	0.4 pg·mL^{-1}	0.001–10 ng·mL^{-1}	[228]
ECL	Lum-AuNPs@g-C_3N_4	tumor exosomes	39 particles μL^{-1}	-	[229]
ECL	g-C_3N_4 NS/TEA/Cu@Cu_2O	microRNA-21	48 aM	-	[230]
ECL	g-C_3N_4/PDDA/CdSe	$VEGF_{165}$	0.68 pg mL^{-1}	2 pg mL^{-1}–2 ng mL^{-1}	[231]

Wu et al. developed an ECL immunosensor to detect the cancer biomarker CA125; nevertheless, its relatively low concentration in human body fluids limits the conventional methods. The disposable and label-free biosensor provided a sensitive detection via ECL emission when multifunctional g-C_3N_4 captures the CA125 tumor marker in the range from 0.001 to 5 U/mL, with a LOD of 0.4 mU/mL [213]. Wang et al. proposed a novel ECL bioassay system for detecting the HL-60 cancer cells based on g-C_3N_4 nanosheets

and Ag–PAMAM–luminol nanocomposites (Ag–PAMAM–luminol NCs), where g-C_3N_4 nanosheets were applied as a reductive–oxidative ECL emitter. The overlapping of the ECL spectrum of g-C_3N_4 nanosheets and the adsorption spectrum of Ag nanoparticles as well as luminol oxidative–reductive ECL emissions simultaneously contributing to the sensitive detection of the HL-60 cancer cells, with 150 cells as the limit of detection [222].

5. Conclusions and Future Perspectives

The early diagnosis of diseases is the best way to improve the treatment prognosis and decrease the side effects of illnesses. Biosensors based on nanomaterials are efficient for this approach due to the high and rapid sensitivity in diagnosing the target molecules that arises from the specific properties of nanomaterials. In recent years, the nanosheets of g-C_3N_4 and their derivatives have attracted a lot of interest owed to their outstanding optical properties (high photoluminescence yield), high surface area, electrical conductivity, antimicrobial activity, and good thermal and chemical stability. Several simple and high-yield methods have been used to synthesize g-C_3N_4-based materials, such as the pyrolysis of low-cost materials, including melamine and urea. C_3N_4-based materials have also been used in various biosensors (SPR, EC, PCL), which demonstrates that they are promising candidates in this field. Moreover, g-C_3N_4-based biosensors show high and rapid sensitivity for detecting diseases, such as cancer; other targets in biological samples; or even the detection of pollutants. Thus, g-C_3N_4 is a new carbon-based 2D nanomaterial for biosensing, and it is expected that in the near future, g-C_3N_4-based biosensors will be improved in order to be more sensitive in diagnosis and functionalized in order to have more selectivity to attach the receptors. We anticipate that further research will be conducted on addressing the intrinsic shortcomings attributed to g-C_3N_4, including poor specific surface area, limited light absorption range, and poor dispersibility in organic and aqueous media.

Author Contributions: Methodology, M.P.; writing-original draft preparation, M.R.-K., F.S.T., N.A., A.S., M.Y. and F.Y.; writing—review and editing, A.R. and A.M.D.-P.; supervision, A.R. and A.M.D.-P. All authors have read and agreed to the published version of the manuscript.

Funding: Financial support from the Community of Madrid within the framework of the multi-year agreement with the University of Alcalá in the line of action "Stimulus to Excellence for Permanent University Professors", Ref. EPU-INV/2020/012, is gratefully acknowledged.

Data Availability Statement: Not available.

Conflicts of Interest: The authors declare that there is no conflict of interest regarding the publication of this article.

Abbreviations

CV	Cyclic Voltammetry
EC	Electrochemical Biosensor
ECL	Electrochemiluminescent Biosensor
FCS	Fluorescence Correlation Spectroscopy
FI	Fluorescence Intensity
FLIM	Fluorescence Lifetime Imaging
FRET	Forster Resonance Energy Transfer
g-C_3N_4	Graphite Phase Carbon Nitride
PCL	Photochemoluminescence Biosensor
SPR	Surface Plasmon Resonance
SPW	Surface Plasmon Wave

References

1. Srinivas, P.R.; Kramer, B.S.; Srivastava, S. Trends in Biomarker Research for Cancer Detection. *Lancet Oncol.* **2001**, *2*, 698–704. [CrossRef]
2. Samadi, A.; Pourmadadi, M.; Yazdian, F.; Rashedi, H.; Navaei-Nigjeh, M.; Eufrasio-da-silva, T. Ameliorating Quercetin Constraints in Cancer Therapy with PH-Responsive Agarose-Polyvinylpyrrolidone -Hydroxyapatite Nanocomposite Encapsulated in Double Nanoemulsion. *Int. J. Biol. Macromol.* **2021**, *182*, 11–25. [CrossRef] [PubMed]
3. Ludwig, J.A.; Weinstein, J.N. Biomarkers in Cancer Staging, Prognosis and Treatment Selection. *Nat. Rev. Cancer* **2005**, *5*, 845–856. [CrossRef] [PubMed]
4. Azimi, S.; Farahani, A.; Sereshti, H. Plasma-functionalized highly aligned CNT-based biosensor for point of care determination of glucose in human blood plasma. *Electroanalysis* **2020**, *32*, 394–403. [CrossRef]
5. Bohunicky, B.; Mousa, S.A. Biosensors: The New Wave in Cancer Diagnosis. *Nanotechnol. Sci. Appl.* **2011**, *4*, 1–10. [CrossRef]
6. Smith, D.S.; Humphrey, P.A.; Catalona, W.J. The Early Detection of Prostate Carcinoma with Prostate Specific Antigen The Washington University Experience. *Cancer* **1997**, *80*, 1852–1856. [CrossRef]
7. Samadi, A.; Yazdian, F.; Navaei-Nigjeh, M.; Rashedi, H. Nanocomposite Hydrogels: A Promising Approach for Developing Stimuli-Responsive Platforms and Their Application in Targeted Drug Delivery. *J. Shahid Sadoughi Univ. Med. Sci.* **2021**, *29*, 3877–3897. [CrossRef]
8. Yazdani, M.; Tavakoli, O.; Khoobi, M.; Wu, Y.S.; Faramarzi, M.A.; Gholibegloo, E.; Farkhondeh, S. Beta-Carotene/Cyclodextrin-Based Inclusion Complex: Improved Loading, Solubility, Stability, and Cytotoxicity. *J. Incl. Phenom. Macrocycl. Chem.* **2022**, *102*, 55–64. [CrossRef]
9. Salehipour, M.; Rezaei, S.; Rezaei, M.; Yazdani, M.; Mogharabi-Manzari, M. Opportunities and Challenges in Biomedical Applications of Metal–Organic Frameworks. *J. Inorg. Organomet. Polym. Mater.* **2021**, *31*, 4443–4462. [CrossRef]
10. Pourmadadi, M.; Dinani, H.S.; Tabar, F.S.; Khassi, K.; Janfaza, S.; Tasnim, N.; Hoorfar, M. Properties and Applications of Graphene and Its Derivatives in Biosensors for Cancer Detection: A Comprehensive Review. *Biosensors* **2022**, *12*, 269. [CrossRef]
11. Samadi, A.; Haseli, S.; Pourmadadi, M.; Rashedi, H.; Yazdian, F.; Navaei-Nigjeh, M. Curcumin-Loaded Chitosan-Agarose-Montmorillonite Hydrogel Nanocomposite for the Treatment of Breast Cancer. In Proceedings of the 2020 27th National and 5th International Iranian Conference on Biomedical Engineering (ICBME), Tehran, Iran, 26 November 2020; pp. 148–153.
12. Haseli, S.; Pourmadadi, M.; Samadi, A.; Yazdian, F.; Abdouss, M.; Rashedi, H.; Navaei-Nigjeh, M. A Novel PH-Responsive Nanoniosomal Emulsion for Sustained Release of Curcumin from a Chitosan-Based Nanocarrier: Emphasis on the Concurrent Improvement of Loading, Sustained Release, and Apoptosis Induction. *Biotechnol. Prog.* **2022**, *38*, e3280. [CrossRef] [PubMed]
13. Pourmadadi, M.; Ahmadi, M.; Abdouss, M.; Yazdian, F.; Rashedi, H.; Navaei-Nigjeh, M.; Hesari, Y. The Synthesis and Characterization of Double Nanoemulsion for Targeted Co-Delivery of 5-Fluorouracil and Curcumin Using PH-Sensitive Agarose/Chitosan Nanocarrier. *J. Drug Deliv. Sci. Technol.* **2022**, *70*, 102849. [CrossRef]
14. Rajabzadeh-Khosroshahi, M.; Pourmadadi, M.; Yazdian, F.; Rashedi, H.; Navaei-Nigjeh, M.; Rasekh, B. Chitosan/Agarose/Graphitic Carbon Nitride Nanocomposite as an Efficient PH-Sensitive Drug Delivery System for Anticancer Curcumin Releasing. *J. Drug Deliv. Sci. Technol.* **2022**, *74*, 103443. [CrossRef]
15. Rahmani, E.; Pourmadadi, M.; Ghorbanian, S.A.; Yazdian, F.; Rashedi, H.; Navaee, M. Preparation of a PH-Responsive Chitosan-Montmorillonite-Nitrogen-Doped Carbon Quantum Dots Nanocarrier for Attenuating Doxorubicin Limitations in Cancer Therapy. *Eng. Life Sci.* **2022**, *22*, 634–649. [CrossRef] [PubMed]
16. Heydari Foroushani, P.H.; Rahmani, E.; Alemzadeh, I.; Vossoughi, M.; Pourmadadi, M.; Rahdar, A.; Díez-Pascual, A.M. Curcumin Sustained Release with a Hybrid Chitosan-Silk Fibroin Nanofiber Containing Silver Nanoparticles as a Novel Highly Efficient Antibacterial Wound Dressing. *Nanomaterials* **2022**, *12*, 3426. [CrossRef] [PubMed]
17. Sugumaran, S.; Jamlos, M.F.; Ahmad, M.N.; Bellan, C.S.; Schreurs, D. Nanostructured Materials with Plasmonic Nanobiosensors for Early Cancer Detection: A Past and Future Prospect. *Biosens. Bioelectron.* **2018**, *100*, 361–373. [CrossRef]
18. Pourmadadi, M.; Yazdian, F.; Hojjati, S.; Khosravi-Darani, K. Detection of Microorganisms Using Graphene-Based Nanobiosensors. *Food Technol. Biotechnol.* **2021**, *59*, 496–506. [CrossRef]
19. Holzinger, M.; Le Goff, A.; Cosnier, S. Nanomaterials for Biosensing Applications: A Review. *Front. Chem.* **2014**, *2*, 63. [CrossRef]
20. Pandey, P.; Datta, M.; Malhotra, B.D. Prospects of Nanomaterials in Biosensors. *Anal. Lett.* **2008**, *41*, 159–209. [CrossRef]
21. Pourmadadi, M.; Nouralishahi, A.; Shalbaf, M.; Shabani Shayeh, J.; Nouralishahi, A. An electrochemical aptasensor fordetection of Prostate-specific antigen-based oncarbon quantum dots-gold nanoparticles. *Biotechnol. Appl. Biochem.* **2022**, 1–9. [CrossRef]
22. Dinani, H.S.; Pourmadadi, M.; Yazdian, F.; Rashedi, H.; Ebrahimi, S.A.S.; Shayeh, J.S.; Ghorbani, M. Fabrication of Au/Fe_3O_4/RGO Based Aptasensor for Measurement of MiRNA-128, a Biomarker for Acute Lymphoblastic Leukemia (ALL). *Eng. Life Sci.* **2022**, *22*, 519–534. [CrossRef] [PubMed]
23. Pourmadadi, M.; Ahmadi, M.J.; Dinani, H.S.; Ajalli, N.; Dorkoosh, F. Theranostic Applications of Stimulus-Responsive Systems Based on Fe_2O_3. *Pharm. Nanotechnol.* **2022**, *10*, 90–112. [CrossRef] [PubMed]
24. Golnaz, M.; Javad, S.; Meysam, S.O.; Mehrab, P.; Fatemeh, Y.; Lobat, T. An electrochemical aptasensor for detection of prostate-specific antigen using reduced graphene gold nanocomposite and cu/carbon quantum dots. *Biotechnol. Appl. Biochem.* **2021**, 1–10. [CrossRef]

25. Zavareh, H.S.; Pourmadadi, M.; Moradi, A.; Yazdian, F.; Omidi, M. Chitosan/Carbon Quantum Dot/Aptamer Complex as a Potential Anticancer Drug Delivery System towards the Release of 5-Fluorouracil. *Int. J. Biol. Macromol.* **2020**, *165*, 1422–1430. [CrossRef] [PubMed]
26. Pourmadadi, M.; Shayeh, J.S.; Arjmand, S.; Omidi, M.; Fatemi, F. An Electrochemical Sandwich Immunosensor of Vascular Endothelial Growth Factor Based on Reduced Graphene Oxide/Gold Nanoparticle Composites. *Microchem. J.* **2020**, *159*, 105476. [CrossRef]
27. Pourmadadi, M.; Shayeh, J.S.; Omidi, M.; Yazdian, F.; Alebouyeh, M.; Tayebi, L. A Glassy Carbon Electrode Modified with Reduced Graphene Oxide and Gold Nanoparticles for Electrochemical Aptasensing of Lipopolysaccharides from *Escherichia coli* Bacteria. *Microchim. Acta* **2019**, *186*, 2–9. [CrossRef] [PubMed]
28. Aayanifard, Z.; Alebrahim, T.; Pourmadadi, M.; Yazdian, F.; Dinani, H.S.; Rashedi, H.; Omidi, M. Ultra PH-Sensitive Detection of Total and Free Prostate-Specific Antigen Using Electrochemical Aptasensor Based on Reduced Graphene Oxide/Gold Nanoparticles Emphasis on TiO_2/Carbon Quantum Dots as a Redox Probe. *Eng. Life Sci.* **2021**, *21*, 739–752. [CrossRef]
29. Behboudi, H.; Mehdipour, G.; Safari, N.; Pourmadadi, M.; Saei, A.; Omidi, M.; Tayebi, L.; Rahmandoust, M. Carbon Quantum Dots in Nanobiotechnology. In *Nanomaterials for Advanced Biological Applications*; Springer: Berlin/Heidelberg, Germany, 2019; pp. 145–179.
30. Kazemi, S.; Pourmadadi, M.; Yazdian, F.; Ghadami, A. The Synthesis and Characterization of Targeted Delivery Curcumin Using Chitosan-Magnetite-Reduced Graphene Oxide as Nano-Carrier. *Int. J. Biol. Macromol.* **2021**, *186*, 554–562. [CrossRef]
31. Malmir, S.; Karbalaei, A.; Pourmadadi, M.; Hamedi, J.; Yazdian, F.; Navaee, M. Antibacterial Properties of a Bacterial Cellulose CQD-TiO_2 Nanocomposite. *Carbohydr. Polym.* **2020**, *234*, 115835. [CrossRef]
32. Zamani, M.; Pourmadadi, M.; Seyyed Ebrahimi, S.A.; Yazdian, F.; Shabani Shayeh, J. A Novel Labeled and Label-Free Dual Electrochemical Detection of Endotoxin Based on Aptamer-Conjugated Magnetic Reduced Graphene Oxide-Gold Nanocomposite. *J. Electroanal. Chem.* **2022**, *908*, 116116. [CrossRef]
33. Azadmanesh, F.; Pourmadadi, M.; Zavar Reza, J.; Yazdian, F.; Omidi, M.; Haghirosadat, B.F. Synthesis of a Novel Nanocomposite Containing Chitosan as a Three-Dimensional Printed Wound Dressing Technique: Emphasis on Gene Expression. *Biotechnol. Prog.* **2021**, *37*, e3132. [CrossRef] [PubMed]
34. Behboodi, H.; Pourmadadi, M.; Omidi, M.; Rahmandoust, M.; Siadat, S.O.R.; Shayeh, J.S. Cu-CDs as Dual Optical and Electrochemical Nanosensor for BME Detection. *Surf. Interfaces* **2022**, *29*, 101710. [CrossRef]
35. Tabar, F.S.; Pourmadadi, M.; Rashedi, H.; Yazdian, F. Design of Electrochemical Nanobiosensor in the Diagnosis of Prostate Specific Antigen (PSA) Using Nanostructures. In Proceedings of the 2020 27th National and 5th International Iranian Conference on Biomedical Engineering (ICBME), Tehran, Iran, 26–27 November 2020; pp. 35–40.
36. Abolghasemzade, S.; Pourmadadi, M.; Rashedi, H.; Yazdian, F.; Kianbakht, S.; Navaei-Nigjeh, M. PVA Based Nanofiber Containing CQDs Modified with Silica NPs and Silk Fibroin Accelerates Wound Healing in a Rat Model. *J. Mater. Chem. B* **2021**, *9*, 658–676. [CrossRef] [PubMed]
37. Kalajahi, S.T.; Mofradnia, S.R.; Yazdian, F.; Rasekh, B.; Neshati, J.; Taghavi, L.; Pourmadadi, M.; Haghirosadat, B.F. Inhibition Performances of Graphene Oxide/Silver Nanostructure for the Microbial Corrosion: Molecular Dynamic Simulation Study. *Environ. Sci. Pollut. Res.* **2022**, *29*, 49884–49897. [CrossRef]
38. Dinani, H.S.; Pourmadadi, M.; Rashedi, H.; Yazdian, F. Fabrication of Nanomaterial-Based Biosensor for Measurement of a MicroRNA Involved in Cancer. In Proceedings of the 2020 27th National and 5th International Iranian Conference on Biomedical Engineering (ICBME), Tehran, Iran, 26–27 November 2020; pp. 47–54.
39. Xiong, M.; Rong, Q.; Meng, H.M.; Zhang, X.B. Two-Dimensional Graphitic Carbon Nitride Nanosheets for Biosensing Applications. *Biosens. Bioelectron.* **2017**, *89*, 212–223. [CrossRef]
40. Duan, F.; Zhang, S.; Yang, L.; Zhang, Z.; He, L.; Wang, M. Bifunctional Aptasensor Based on Novel Two-Dimensional Nanocomposite of MoS_2 Quantum Dots and g-C_3N_4 Nanosheets Decorated with Chitosan-Stabilized Au Nanoparticles for Selectively Detecting Prostate Specific Antigen. *Anal. Chim. Acta* **2018**, *1036*, 121–132. [CrossRef]
41. Naderian, N.; Pourmadadi, M.; Rashedi, H.; Yazdian, F. Design of a Novel Nanobiosensor for the Diagnosis of Acute Lymphoid Leukemia (ALL) by Measurement of MiRNA-128. In Proceedings of the 2020 27th National and 5th International Iranian Conference on Biomedical Engineering (ICBME), Tehran, Iran, 26–27 November 2020; pp. 41–46.
42. Sakthivel, A.; Chandrasekaran, A.; Sadasivam, M.; Manickam, P.; Alwarappan, S. Sulphur Doped Graphitic Carbon Nitride as a Dual Biosensing Platform for the Detection of Cancer Biomarker CA15-3. *J. Electrochem. Soc* **2021**, *168*, 017507. [CrossRef]
43. Ismael, M. A Review on Graphitic Carbon Nitride (g-C_3N_4) Based Nanocomposites: Synthesis, Categories, and Their Application in Photocatalysis. *J. Alloys Compd.* **2020**, *846*, 156446. [CrossRef]
44. Wang, H.; Qi, C.; He, W.; Wang, M.; Jiang, W.; Yin, H.; Ai, S. A Sensitive Photoelectrochemical Immunoassay of N6-Methyladenosine Based on Dual-Signal Amplification Strategy: Ru Doped in SiO_2 Nanosphere and Carboxylated g-C_3N_4. *Biosens. Bioelectron.* **2018**, *99*, 281–288. [CrossRef]
45. Feng, L.; He, F.; Liu, B.; Yang, G.; Gai, S.; Yang, P.; Li, C.; Dai, Y.; Lv, R.; Lin, J. G-C_3N_4 Coated Upconversion Nanoparticles for 808 Nm Near-Infrared Light Triggered Phototherapy and Multiple Imaging. *Chem. Mater.* **2016**, *28*, 7935–7946. [CrossRef]
46. Zhang, X.; Xie, X.; Wang, H.; Zhang, J.; Pan, B.; Xie, Y. Enhanced Photoresponsive Ultrathin Graphitic-Phase C3N 4 Nanosheets for Bioimaging. *J. Am. Chem. Soc.* **2013**, *135*, 18–21. [CrossRef] [PubMed]

47. Zhang, M.; Wang, Q.; Xu, Y.; Guo, L.; Lai, Z.; Li, Z. Graphitic Carbon Nitride Quantum Dots as Analytical Probe for Viewing Sialic Acid on the Surface of Cells and Tissues. *Anal. Chim. Acta* **2020**, *1095*, 204–211. [CrossRef] [PubMed]
48. Chen, L.; Huang, D.; Ren, S.; Dong, T.; Chi, Y.; Chen, G. Preparation of Graphite-like Carbon Nitride Nanoflake Film with Strong Fluorescent and Electrochemiluminescent Activity. *Nanoscale* **2013**, *5*, 225–230. [CrossRef] [PubMed]
49. Ong, W.J.; Tan, L.L.; Ng, Y.H.; Yong, S.T.; Chai, S.P. Graphitic Carbon Nitride (g-C_3N_4)-Based Photocatalysts for Artificial Photosynthesis and Environmental Remediation: Are We a Step Closer to Achieving Sustainability? *Chem. Rev.* **2016**, *116*, 7159–7329. [CrossRef]
50. Vasiljević, J.; Jerman, I.; Simončič, B. Graphitic Carbon Nitride as a New Sustainable Photocatalyst for Textile Functionalization. *Polymers* **2021**, *13*, 2568. [CrossRef]
51. Alwin, E.; Kočí, K.; Wojcieszak, R.; Zieliński, M.; Edelmannová, M.; Pietrowski, M. Influence of High Temperature Synthesis on the Structure of Graphitic Carbon Nitride and Its Hydrogen Generation Ability. *Materials* **2020**, *13*, 2756. [CrossRef]
52. Thomas, A.; Fischer, A.; Goettmann, F.; Antonietti, M.; Müller, J.O.; Schlögl, R.; Carlsson, J.M. Graphitic Carbon Nitride Materials: Variation of Structure and Morphology and Their Use as Metal-Free Catalysts. *J. Mater. Chem.* **2008**, *18*, 4893–4908. [CrossRef]
53. Tian, C.; Zhao, H.; Sun, H.; Xiao, K.; Keung Wong, P. Enhanced Adsorption and Photocatalytic Activities of Ultrathin Graphitic Carbon Nitride Nanosheets: Kinetics and Mechanism. *Chem. Eng. J.* **2020**, *381*, 122760. [CrossRef]
54. Du, X.; Kleitz, F.; Li, X.; Huang, H.; Zhang, X.; Qiao, S.Z. Disulfide-Bridged Organosilica Frameworks: Designed, Synthesis, Redox-Triggered Biodegradation, and Nanobiomedical Applications. *Adv. Funct. Mater.* **2018**, *28*, 1707325. [CrossRef]
55. Dante, R.C.; Trakulmututa, J.; Meejoo-Smith, S.; Sirisit, N.; Martín-Ramos, P.; Chamorro-Posada, P.; Rutto, D.; Dante, D.G. A Solid-State Glucose Sensor Based on Cu and Fe–Doped Carbon Nitride. *Mater. Chem. Phys.* **2021**, *258*, 124023. [CrossRef]
56. Ma, T.Y.; Tang, Y.; Dai, S.; Qiao, S.Z. Proton-Functionalized Two-Dimensional Graphitic Carbon Nitride Nanosheet: An Excellent Metal-/Label-Free Biosensing Platform. *Small* **2014**, *10*, 2382–2389. [CrossRef] [PubMed]
57. Zheng, Y.; Lin, L.; Wang, B.; Wang, X. Graphitic Carbon Nitride Polymers toward Sustainable Photoredox Catalysis. *Angew. Chem.-Int. Ed.* **2015**, *54*, 12868–12884. [CrossRef] [PubMed]
58. Liao, G.; He, F.; Li, Q.; Zhong, L.; Zhao, R.; Che, H.; Gao, H.; Fang, B. Emerging Graphitic Carbon Nitride-Based Materials for Biomedical Applications. *Prog. Mater. Sci.* **2020**, *112*, 100666. [CrossRef]
59. Wang, A.J.; Li, H.; Huang, H.; Qian, Z.S.; Feng, J.J. Fluorescent Graphene-like Carbon Nitrides: Synthesis, Properties and Applications. *J. Mater. Chem. C* **2016**, *4*, 8146–8160. [CrossRef]
60. Reddy, K.R.; Reddy, C.V.; Nadagouda, M.N.; Shetti, N.P.; Jaesool, S.; Aminabhavi, T.M. Polymeric Graphitic Carbon Nitride (g-C_3N_4)-Based Semiconducting Nanostructured Materials: Synthesis Methods, Properties and Photocatalytic Applications. *J. Environ. Manag.* **2019**, *238*, 25–40. [CrossRef]
61. Yu, H.; Shi, R.; Zhao, Y.; Waterhouse, G.I.N.; Wu, L.Z.; Tung, C.H.; Zhang, T. Smart Utilization of Carbon Dots in Semiconductor Photocatalysis. *Adv. Mater.* **2016**, *28*, 9454–9477. [CrossRef]
62. Hatamie, A.; Marahel, F.; Sharifat, A. Green Synthesis of Graphitic Carbon Nitride Nanosheet (g-C_3N_4) and Using It as a Label-Free Fluorosensor for Detection of Metronidazole via Quenching of the Fluorescence. *Talanta* **2018**, *176*, 518–525. [CrossRef]
63. Wang, L.; Wang, C.; Hu, X.; Xue, H.; Pang, H. Metal/Graphitic Carbon Nitride Composites: Synthesis, Structures, and Applications. *Chem.-Asian J.* **2016**, *11*, 3305–3328. [CrossRef]
64. Vinoth, S.; Ramaraj, R.; Pandikumar, A. Facile Synthesis of Calcium Stannate Incorporated Graphitic Carbon Nitride Nanohybrid Materials: A Sensitive Electrochemical Sensor for Determining Dopamine. *Mater. Chem. Phys.* **2020**, *245*, 122743. [CrossRef]
65. Imran, H.; Manikandan, P.N.; Dharuman, V. Highly Selective and Rapid Non-Enzymatic Glucose Sensing at Ultrathin Layered Nb Doped C_3N_4 for Extended Linearity Range. *Microchem. J.* **2021**, *160*, 105774. [CrossRef]
66. Vinoth, S.; Sampathkumar, P.; Giribabu, K.; Pandikumar, A. Ultrasonically Assisted Synthesis of Barium Stannate Incorporated Graphitic Carbon Nitride Nanocomposite and Its Analytical Performance in Electrochemical Sensing of 4-Nitrophenol. *Ultrason. Sonochem.* **2020**, *62*, 104855. [CrossRef] [PubMed]
67. Lewandowski, C.M. Surface Plasmon Resonance (SPR) Biosensor Development. *Eff. Br. Mindfulness Interv. Acute Pain Exp. Exam. Individ. Differ.* **2015**, *1*, 43–48.
68. Nie, W.; Wang, Q.; Zou, L.; Zheng, Y.; Liu, X.; Yang, X.; Wang, K. Low-Fouling Surface Plasmon Resonance Sensor for Highly Sensitive Detection of MicroRNA in a Complex Matrix Based on the DNA Tetrahedron. *Anal. Chem.* **2018**, *90*, 12584–12591. [CrossRef]
69. Ho, A.H.P.; Kim, D.; Somekh, M.G. *Handbook of Photonics for Biomedical Engineering*; Springer: Berlin/Heidelberg, Germany, 2017; pp. 1–947. [CrossRef]
70. Yao, Y.; Yi, B.; Xiao, J.; Li, Z.H. Surface Plasmon Resonance Biosensors and Its Application. In Proceedings of the 2007 1st International Conference on Bioinformatics and Biomedical Engineering, Wuhan, China, 6–8 July 2007; pp. 1043–1046. [CrossRef]
71. Maurya, J.B.; Prajapati, Y.K. A Comparative Study of Different Metal and Prism in the Surface Plasmon Resonance Biosensor Having MoS_2-Graphene. *Opt. Quantum Electron.* **2016**, *48*, 1–12. [CrossRef]
72. Miyazaki, C.M.; Shimizu, F.M.; Ferreira, M. *Surface Plasmon Resonance (SPR) for Sensors and Biosensors*; Elsevier Inc.: Amsterdam, The Netherlands, 2017; ISBN 9780323497794.
73. Lin, C.; Chen, S. Design of High-Performance Au-Ag-Dielectric-Graphene Based Surface Plasmon Resonance Biosensors Using Genetic Algorithm. *J. Appl. Phys.* **2019**, *125*, 113101. [CrossRef]

74. Homola, J. Surface Plasmon Resonance Sensors for Detection of Chemical and Biological Species. *Chem. Rev.* **2008**, *108*, 462–493. [CrossRef]
75. Boozer, C.; Kim, G.; Cong, S.; Guan, H.W.; Londergan, T. Looking towards Label-Free Biomolecular Interaction Analysis in a High-Throughput Format: A Review of New Surface Plasmon Resonance Technologies. *Curr. Opin. Biotechnol.* **2006**, *17*, 400–405. [CrossRef]
76. Gao, Y.; Liu, M.; Zhang, Y.; Liu, Z.; Yang, Y.; Zhao, L. Recent Development on Narrow Bandgap Conjugated Polymers for Polymer Solar Cells. *Polymers* **2017**, *9*, 39. [CrossRef]
77. Topkaya, S.N.; Azimzadeh, M.; Ozsoz, M. Electrochemical Biosensors for Cancer Biomarkers Detection: Recent Advances and Challenges. *Electroanalysis* **2016**, *28*, 1402–1419. [CrossRef]
78. Taniselass, S.; Arshad, M.K.M.; Gopinath, S.C.B. Graphene-Based Electrochemical Biosensors for Monitoring Noncommunicable Disease Biomarkers. *Biosens. Bioelectron.* **2019**, *130*, 276–292. [CrossRef]
79. Gan, T.; Shi, Z.; Sun, J.; Liu, Y. Simple and Novel Electrochemical Sensor for the Determination of Tetracycline Based on Iron/Zinc Cations-Exchanged Montmorillonite Catalyst. *Talanta* **2014**, *121*, 187–193. [CrossRef]
80. Cho, I.H.; Kim, D.H.; Park, S. Electrochemical Biosensors: Perspective on Functional Nanomaterials for on-Site Analysis. *Biomater. Res.* **2020**, *24*, 1–12. [CrossRef]
81. Li, Y.P.; Cao, H.B.; Liu, C.M.; Zhang, Y. Electrochemical Reduction of Nitrobenzene at Carbon Nanotube Electrode. *J. Hazard. Mater.* **2007**, *148*, 158–163. [CrossRef] [PubMed]
82. Patnaik, S.; Martha, S.; Acharya, S.; Parida, K.M. An Overview of the Modification of G-C_3N_4 with High Carbon Containing Materials for Photocatalytic Applications. *Inorg. Chem. Front.* **2016**, *3*, 336–347. [CrossRef]
83. Fang, T.; Yang, X.; Zhang, L.; Gong, J. Ultrasensitive Photoelectrochemical Determination of Chromium(VI) in Water Samples by Ion-Imprinted/Formate Anion-Incorporated Graphitic Carbon Nitride Nanostructured Hybrid. *J. Hazard. Mater.* **2016**, *312*, 106–113. [CrossRef] [PubMed]
84. Wang, X.; Maeda, K.; Thomas, A.; Takanabe, K.; Xin, G.; Carlsson, J.M.; Domen, K.; Antonietti, M. A Metal-Free Polymeric Photocatalyst for Hydrogen Production from Water under Visible Light. *Nat. Mater.* **2009**, *8*, 76–80. [CrossRef]
85. Zhao, Q.; Wu, W.; Wei, X.; Jiang, S.; Zhou, T.; Li, Q.; Lu, Q. Graphitic Carbon Nitride as Electrode Sensing Material for Tetrabromobisphenol-A Determination. *Sens. Actuators B Chem.* **2017**, *248*, 673–681. [CrossRef]
86. Kathiresan, V.; Rajarathinam, T.; Lee, S.; Kim, S.; Lee, J.; Thirumalai, D.; Chang, S.C. Cost-Effective Electrochemical Activation of Graphitic Carbon Nitride on the Glassy Carbon Electrode Surface for Selective Determination of Serotonin. *Sensors* **2020**, *20*, 6083. [CrossRef]
87. Zhan, T.; Tian, X.; Ding, G.; Liu, X.; Wang, L.; Teng, H. Quaternarization Strategy to Ultrathin Lamellar Graphitic C_3N_4 Ionic Liquid Nanostructure for Enhanced Electrochemical 2,4-Dichlorophenol Sensing. *Sens. Actuators B Chem.* **2019**, *283*, 463–471. [CrossRef]
88. Miao, J.; Li, X.; Li, Y.; Dong, X.; Zhao, G.; Fang, J.; Wei, Q.; Cao, W. Dual-Signal Sandwich Electrochemical Immunosensor for Amyloid β-Protein Detection Based on Cu–Al_2O_3-g–C_3N_4–Pd and UiO-66@PANI-MB. *Anal. Chim. Acta* **2019**, *1089*, 48–55. [CrossRef]
89. Ansari, S.; Ansari, M.S.; Devnani, H.; Satsangee, S.P.; Jain, R. CeO_2/g-C_3N_4 Nanocomposite: A Perspective for Electrochemical Sensing of Anti-Depressant Drug. *Sens. Actuators B Chem.* **2018**, *273*, 1226–1236. [CrossRef]
90. Li, C.; Xu, J.; Wu, Y.; Zhang, Y.; Zhang, C.; Lei, W.; Hao, Q. G-C_3N_4 Nanofibers Doped Poly(3,4-Ethylenedioxythiophene) Modified Electrode for Simultaneous Determination of Ascorbic Acid and Acetaminophen. *J. Electroanal. Chem.* **2018**, *824*, 52–59. [CrossRef]
91. Zhou, D.; Wang, M.; Dong, J.; Ai, S. A Novel Electrochemical Immunosensor Based on Mesoporous Graphitic Carbon Nitride for Detection of Subgroup J of Avian Leukosis Viruses. *Electrochim. Acta* **2016**, *205*, 95–101. [CrossRef]
92. Yan, K.; Yang, Y.; Zhang, J. A Self-Powered Sensor Based on Molecularly Imprinted Polymer-Coupled Graphitic Carbon Nitride Photoanode for Selective Detection of Bisphenol A. *Sens. Actuators B Chem.* **2018**, *259*, 394–401. [CrossRef]
93. Sun, A.L.; Qi, Q.A. Silver-Functionalized g-C_3N_4 Nanohybrids as Signal-Transduction Tags for Electrochemical Immunoassay of Human Carbohydrate Antigen 19-9. *Analyst* **2016**, *141*, 4366–4372. [CrossRef]
94. Afzali, M.; Shafiee, M.R.M.; Parhizkar, J. Au Nanorods/ g-C_3N_4 Composite Based Biosensor for Electrochemical Detection of Chronic Lymphocytic Leukemia. *Nanomed. Res. J.* **2020**, *5*, 32–43. [CrossRef]
95. Chen, X.; Ke, X.X.; Liu, Y.; Weerasooriya, R.; Li, H.; Wu, Y.C. Photocatalytically Induced Au/Mpg-C_3N_4 Nanocomposites for Robust Electrochemical Detection of Cr(VI) in Tannery Wastewater. *J. Environ. Chem. Eng.* **2020**, *9*, 104642. [CrossRef]
96. Xiao, F.; Li, H.; Yan, X.; Yan, L.; Zhang, X.; Wang, M.; Qian, C.; Wang, Y. Graphitic Carbon Nitride/Graphene Oxide(g-C_3N_4/GO) Nanocomposites Covalently Linked with Ferrocene Containing Dendrimer for Ultrasensitive Detection of Pesticide. *Anal. Chim. Acta* **2020**, *1103*, 84–96. [CrossRef]
97. Xu, Y.; Lei, W.; Su, J.; Hu, J.; Yu, X.; Zhou, T.; Yang, Y.; Mandler, D.; Hao, Q. A High-Performance Electrochemical Sensor Based on g-C_3N_4-E-PEDOT for the Determination of Acetaminophen. *Electrochim. Acta* **2018**, *259*, 994–1003. [CrossRef]
98. Kesavan, G.; Chen, S.M. Highly Sensitive Electrochemical Sensor Based on Carbon-Rich Graphitic Carbon Nitride as an Electrocatalyst for the Detection of Diphenylamine. *Microchem. J.* **2020**, *159*, 105587. [CrossRef]
99. Zou, J.; Wu, S.; Liu, Y.; Sun, Y.; Cao, Y.; Hsu, J.P.; Shen Wee, A.T.; Jiang, J. An Ultra-Sensitive Electrochemical Sensor Based on 2D g-C_3N_4/CuO Nanocomposites for Dopamine Detection. *Carbon N. Y.* **2018**, *130*, 652–663. [CrossRef]

100. Ponnaiah, S.K.; Prakash, P.; Muthupandian, S. Ultrasonic Energy-Assisted in-Situ Synthesis of Ru0/PANI/g-C_3N_4 Nanocomposite: Application for Picomolar-Level Electrochemical Detection of Endocrine Disruptor (Bisphenol-A) in Humans and Animals. *Ultrason. Sonochem.* **2019**, *58*, 104629. [CrossRef] [PubMed]
101. Sun, Y.; Jiang, J.; Liu, Y.; Wu, S.; Zou, J. A Facile One-Pot Preparation of Co_3O_4/g-C_3N_4 Heterojunctions with Excellent Electrocatalytic Activity for the Detection of Environmental Phenolic Hormones. *Appl. Surf. Sci.* **2018**, *430*, 362–370. [CrossRef]
102. Karthika, A.; Suganthi, A.; Rajarajan, M. An In-Situ Synthesis of Novel V_2O_5/G-C_3N_4/PVA Nanocomposite for Enhanced Electrocatalytic Activity toward Sensitive and Selective Sensing of Folic Acid in Natural Samples. *Arab. J. Chem.* **2020**, *13*, 3639–3652. [CrossRef]
103. Kokulnathan, T.; Wang, T.-J. Vanadium Carbide-Entrapped Graphitic Carbon Nitride Nanocomposites: Synthesis and Electrochemical Platforms for Accurate Detection of Furazolidone. *ACS Appl. Nano Mater.* **2020**, *3*, 2554–2561. [CrossRef]
104. Balasubramanian, P.; Annalakshmi, M.; Chen, S.M.; Chen, T.W. Sonochemical Synthesis of Molybdenum Oxide (MoO_3) Microspheres Anchored Graphitic Carbon Nitride (g-C_3N_4) Ultrathin Sheets for Enhanced Electrochemical Sensing of Furazolidone. *Ultrason. Sonochem.* **2019**, *50*, 96–104. [CrossRef]
105. Yola, M.L.; Atar, N. Amperometric Galectin-3 Immunosensor-Based Gold Nanoparticle-Functionalized Graphitic Carbon Nitride Nanosheets and Core-Shell Ti-MOF@COFs Composites. *Nanoscale* **2020**, *12*, 19824–19832. [CrossRef]
106. Zeng, G.; Duan, M.; Xu, Y.; Ge, F.; Wang, W. Platinum (II)-Doped Graphitic Carbon Nitride with Enhanced Peroxidase-like Activity for Detection of Glucose and H_2O_2. *Spectrochim. Acta-Part A Mol. Biomol. Spectrosc.* **2020**, *241*, 118649. [CrossRef]
107. Tian, K.J.; Liu, H.; Dong, Y.P.; Chu, X.F.; Wang, S.B. Amperometric Detection of Glucose Based on Immobilizing Glucose Oxidase on G-C_3N_4 Nanosheets. *Colloids Surf. A Physicochem. Eng. Asp.* **2019**, *581*, 123808. [CrossRef]
108. Liu, L.; Wang, M.; Wang, C. In-Situ Synthesis of Graphitic Carbon Nitride/Iron Oxide−copper Composites and Their Application in the Electrochemical Detection of Glucose. *Electrochim. Acta* **2018**, *265*, 275–283. [CrossRef]
109. Amiri, M.; Salehniya, H.; Habibi-Yangjeh, A. Graphitic Carbon Nitride/Chitosan Composite for Adsorption and Electrochemical Determination of Mercury in Real Samples. *Ind. Eng. Chem. Res.* **2016**, *55*, 8114–8122. [CrossRef]
110. Ganjali, M.R.; Rahmani, A.R.; Shokoohi, R.; Farmany, A.; Khazaei, M. A Highly Sensitive and Selective Electrochemical Mercury(II) Sensor Based on Nanoparticles of Hg(II)-Imprinted Polymer and Graphitic Carbon Nitride (g-C_3N_4). *Int. J. Electrochem. Sci.* **2019**, *14*, 6420–6430. [CrossRef]
111. Mahmoudian, M.R.; Basirun, W.J.; Alias, Y.; MengWoi, P. Investigating the Effectiveness of G-C_3N_4 on Pt /g-C_3N_4/ Polythiophene Nanocomposites Performance as an Electrochemical Sensor for Hg^{2+} Detection. *J. Environ. Chem. Eng.* **2020**, *8*, 104204. [CrossRef]
112. Zhang, J.; Zhu, Z.; Di, J.; Long, Y.; Li, W.; Tu, Y. A Sensitive Sensor for Trace Hg2+ Determination Based on Ultrathin G-C_3N_4 Modified Glassy Carbon Electrode. *Electrochim. Acta* **2015**, *186*, 192–200. [CrossRef]
113. Sun, C.; Zhang, M.; Fei, Q.; Wang, D.; Sun, Z.; Geng, Z.; Xu, W.; Liu, F. Graphite-like g-C_3N_4-F127-Au Nanosheets Used for Sensitive Monitoring of Heat Shock Protein 90. *Sens. Actuators B Chem.* **2018**, *256*, 160–166. [CrossRef]
114. Dai, G.; Xie, J.; Li, C.; Liu, S. Flower-like Co3O4/Graphitic Carbon Nitride Nanocomposite Based Electrochemical Sensor and Its Highly Sensitive Electrocatalysis of Hydrazine. *J. Alloys Compd.* **2017**, *727*, 43–51. [CrossRef]
115. Mohammad, A.; Khan, M.E.; Cho, M.H. Sulfur-Doped-Graphitic-Carbon Nitride (S-g-C_3N_4) for Low Cost Electrochemical Sensing of Hydrazine. *J. Alloys Compd.* **2020**, *816*, 152522. [CrossRef]
116. Afshari, M.; Dinari, M.; Momeni, M.M. The Graphitic Carbon Nitride/Polyaniline/Silver Nanocomposites as a Potential Electrocatalyst for Hydrazine Detection. *J. Electroanal. Chem.* **2019**, *833*, 9–16. [CrossRef]
117. Dai, G.; Xie, J.; Li, C.; Liu, S. A Highly Sensitive Non-Enzymatic Sensor Based on a Cu/MnO_2/g-C_3N_4-Modified Glassy Carbon Electrode for the Analysis of Hydrogen Peroxide Residues in Food Samples. *Aust. J. Chem.* **2017**, *70*, 1118–1126. [CrossRef]
118. Mohammad, A.; Khan, M.E.; Yoon, T.; Hwan Cho, M. Na,O-Co-Doped-Graphitic-Carbon Nitride (Na,O-g-C_3N_4) for Nonenzymatic Electrochemical Sensing of Hydrogen Peroxide. *Appl. Surf. Sci.* **2020**, *525*, 146353. [CrossRef]
119. Gomez, C.G.; Silva, A.M.; Strumia, M.C.; Avalle, L.B.; Rojas, M.I. The Origin of High Electrocatalytic Activity of Hydrogen Peroxide Reduction Reaction by a G-C_3N_4/HOPG Sensor. *Nanoscale* **2017**, *9*, 11170–11179. [CrossRef] [PubMed]
120. Fu, R.; Yu, P.; Wang, M.; Sun, J.; Chen, D.; Jin, C.; Li, Z. The Research of Lead Ion Detection Based on RGO/g-C_3N_4 Modified Glassy Carbon Electrode. *Microchem. J.* **2020**, *157*, 105076. [CrossRef]
121. Wang, M.; Liu, C.; Zhang, X.; Fan, Z.; Xu, J.; Tong, Z. In Situ Synthesis of $CsTi_2NbO_7$@g-C_3N_4 Core-Shell Heterojunction with Excellent Electrocatalytic Performance for the Detection of Nitrite. *J. Mater. Res.* **2018**, *33*, 3936–3945. [CrossRef]
122. Vinoth, S.; Mary Rajaitha, P.; Pandikumar, A. In-Situ Pyrolytic Processed Zinc Stannate Incorporated Graphitic Carbon Nitride Nanocomposite for Selective and Sensitive Electrochemical Determination of Nitrobenzene. *Compos. Sci. Technol.* **2020**, *195*, 108192. [CrossRef]
123. Rana, A.; Killa, M.; Yadav, N.; Mishra, A.; Mathur, A.; Kumar, A.; Khanuja, M.; Narang, J.; Pilloton, R. Graphitic Carbon Nitride as an Amplification Platform on an Electrochemical Paper-Based Device for the Detection of Norovirus-Specific DNA. *Sensors* **2020**, *20*, 2070. [CrossRef]
124. Zhu, X.; Kou, F.; Xu, H.; Han, Y.; Yang, G.; Huang, X.; Chen, W.; Chi, Y.; Lin, Z. Label-Free Ochratoxin A Electrochemical Aptasensor Based on Target-Induced Noncovalent Assembly of Peroxidase-like Graphitic Carbon Nitride Nanosheet. *Sens. Actuators B Chem.* **2018**, *270*, 263–269. [CrossRef]

125. Wang, B.; Ye, C.; Zhong, X.; Chai, Y.; Chen, S.; Yuan, R. Electrochemical Biosensor for Organophosphate Pesticides and Huperzine-A Detection Based on Pd Wormlike Nanochains/Graphitic Carbon Nitride Nanocomposites and Acetylcholinesterase. *Electroanalysis* **2016**, *28*, 304–311. [CrossRef]
126. Alizadeh, T.; Nayeri, S.; Hamidi, N. Graphitic Carbon Nitride (g-C_3N_4)/Graphite Nanocomposite as an Extraordinarily Sensitive Sensor for Sub-Micromolar Detection of Oxalic Acid in Biological Samples. *RSC Adv.* **2019**, *9*, 13096–13103. [CrossRef]
127. Yan, Y.; Jamal, R.; Yu, Z.; Zhang, R.; Zhang, W.; Ge, Y.; Liu, Y.; Abdiryim, T. Composites of Thiol-Grafted PEDOT with N-Doped Graphene or Graphitic Carbon Nitride as an Electrochemical Sensor for the Detection of Paracetamol. *J. Mater. Sci.* **2020**, *55*, 5571–5586. [CrossRef]
128. Zou, J.; Deng, W.; Jiang, J.; Arramel; He, X.; Li, N.; Fang, J.; Hsu, J.P. Built-in Electric Field-Assisted Step-Scheme Heterojunction of Carbon Nitride-Copper Oxide for Highly Selective Electrochemical Detection of p-Nonylphenol. *Electrochim. Acta* **2020**, *354*, 136658. [CrossRef]
129. Zhou, X.; Yang, L.; Tan, X.; Zhao, G.; Xie, X.; Du, G. A Robust Electrochemical Immunosensor Based on Hydroxyl Pillar[5]Arene@AuNPs@g-C_3N_4 Hybrid Nanomaterial for Ultrasensitive Detection of Prostate Specific Antigen. *Biosens. Bioelectron.* **2018**, *112*, 31–39. [CrossRef] [PubMed]
130. Ding, L.L.; Ge, J.P.; Zhou, W.Q.; Gao, J.P.; Zhang, Z.Y.; Xiong, Y. Nanogold-Functionalized g-C_3N_4 Nanohybrids for Sensitive Impedimetric Immunoassay of Prostate-Specific Antigen Using Enzymatic Biocatalytic Precipitation. *Biosens. Bioelectron.* **2016**, *85*, 212–219. [CrossRef] [PubMed]
131. Selvarajan, S.; Suganthi, A.; Rajarajan, M. Fabrication of G-C_3N_4/NiO Heterostructured Nanocomposite Modified Glassy Carbon Electrode for Quercetin Biosensor. *Ultrason. Sonochem.* **2018**, *41*, 651–660. [CrossRef]
132. Mahmoudian, M.R.; Alias, Y.; Meng Woi, P.; Yousefi, R.; Basirun, W.J. An Electrochemical Sensor Based on Pt/g-C_3N_4/Polyaniline Nanocomposite for Detection of Hg2+. *Adv. Powder Technol.* **2020**, *31*, 3372–3380. [CrossRef]
133. Rajaji, U.; Chen, T.W.; Chinnapaiyan, S.; Chen, S.M.; Govindasamy, M. Two-Dimensional Binary Nanosheets (Bi_2Te_3@g-C_3N_4): Application toward the Electrochemical Detection of Food Toxic Chemical. *Anal. Chim. Acta* **2020**, *1125*, 220–230. [CrossRef]
134. Li, M.; He, B. Ultrasensitive Sandwich-Type Electrochemical Biosensor Based on Octahedral Gold Nanoparticles Modified Poly (Ethylenimine) Functionalized Graphitic Carbon Nitride Nanosheets for the Determination of Sulfamethazine. *Sens. Actuators B Chem.* **2021**, *329*, 129158. [CrossRef]
135. Chen, J.; Liu, Y.; Zhao, G.C. A Novel Photoelectrochemical Biosensor for Tyrosinase and Thrombin Detection. *Sensors* **2016**, *16*, 135. [CrossRef]
136. Devadoss, A.; Sudhagar, P.; Terashima, C.; Nakata, K.; Fujishima, A. Photoelectrochemical Biosensors: New Insights into Promising Photoelectrodes and Signal Amplification Strategies. *J. Photochem. Photobiol. C Photochem. Rev.* **2015**, *24*, 43–63. [CrossRef]
137. Abolhasan, R.; Mehdizadeh, A.; Rashidi, M.R.; Aghebati-Maleki, L.; Yousefi, M. Application of Hairpin DNA-Based Biosensors with Various Signal Amplification Strategies in Clinical Diagnosis. *Biosens. Bioelectron.* **2019**, *129*, 164–174. [CrossRef]
138. Forster, R.J.; Bertoncello, P.; Keyes, T.E. Electrogenerated Chemiluminescence. *Annu. Rev. Anal. Chem.* **2009**, *2*, 359–385. [CrossRef]
139. Zhao, W.W.; Xu, J.J.; Chen, H.Y. Photoelectrochemical Immunoassays. *Anal. Chem.* **2018**, *90*, 615–627. [CrossRef]
140. Victorious, A.; Saha, S.; Pandey, R.; Didar, T.F.; Soleymani, L. Affinity-Based Detection of Biomolecules Using Photo-Electrochemical Readout. *Front. Chem.* **2019**, *7*, 617. [CrossRef]
141. Zou, X.; Sun, Z.; Hu, Y.H. G-C_3N_4-Based Photoelectrodes for Photoelectrochemical Water Splitting: A Review. *J. Mater. Chem. A* **2020**, *8*, 21474–21502. [CrossRef]
142. Zang, Y.; Ju, Y.; Hu, X.; Zhou, H.; Yang, Z.; Jiang, J.; Xue, H. WS_2 Nanosheets-Sensitized CdS Quantum Dots Heterostructure for Photoelectrochemical Immunoassay of Alpha-Fetoprotein Coupled with Enzyme-Mediated Biocatalytic Precipitation. *Analyst* **2018**, *143*, 2895–2900. [CrossRef] [PubMed]
143. Pang, X.; Pan, J.; Gao, P.; Wang, Y.; Wang, L.; Du, B.; Wei, Q. A Visible Light Induced Photoelectrochemical Aptsensor Constructed by Aligned ZnO@CdTe Core Shell Nanocable Arrays/Carboxylated g-C_3N_4 for the Detection of Proprotein Convertase Subtilisin/Kexin Type 6 Gene. *Biosens. Bioelectron.* **2015**, *74*, 49–58. [CrossRef] [PubMed]
144. Sui, C.; Li, F.; Wu, H.; Yin, H.; Zhang, S.; Waterhouse, G.I.N.; Wang, J.; Zhu, L.; Ai, S. Photoelectrochemical Biosensor for 5hmC Detection Based on the Photocurrent Inhibition Effect of ZnO on MoS_2/C_3N_4 Heterojunction. *Biosens. Bioelectron.* **2019**, *142*, 111516. [CrossRef] [PubMed]
145. Mao, L.; Xue, X.; Xu, X.; Wen, W.; Chen, M.M.; Zhang, X.; Wang, S. Heterostructured CuO-g-C_3N_4 Nanocomposites as a Highly Efficient Photocathode for Photoelectrochemical Aflatoxin B1 Sensing. *Sens. Actuators B Chem.* **2021**, *329*, 129146. [CrossRef]
146. Wang, F.X.; Ye, C.; Mo, S.; Liao, L.L.; Zhang, X.F.; Ling, Y.; Lu, L.; Luo, H.Q.; Li, N.B. A Novel "Signal-on" Photoelectrochemical Sensor for Ultrasensitive Detection of Alkaline Phosphatase Activity Based on a TiO_2/g-C_3N_4 Heterojunction. *Analyst* **2018**, *143*, 3399–3407. [CrossRef]
147. Sui, C.; Zhou, Y.; Wang, M.; Yin, H.; Wang, P.; Ai, S. Aptamer-Based Photoelectrochemical Biosensor for Antibiotic Detection Using Ferrocene Modified DNA as Both Aptamer and Electron Donor. *Sens. Actuators B Chem.* **2018**, *266*, 514–521. [CrossRef]
148. Kang, Q.; Wang, X.; Ma, X.; Kong, L.; Zhang, P.; Shen, D. Sensitive Detection of Ascorbic Acid and Alkaline Phosphatase Activity by Double-Channel Photoelectrochemical Detection Design Based on g-C_3N_4/TiO_2 Nanotubes Hybrid Film. *Sens. Actuators B Chem.* **2016**, *230*, 231–241. [CrossRef]

149. Sun, B.; Dong, J.; Cui, L.; Feng, T.; Zhu, J.; Liu, X.; Ai, S. A Dual Signal-on Photoelectrochemical Immunosensor for Sensitively Detecting Target Avian Viruses Based on AuNPs/g-C_3N_4 Coupling with CdTe Quantum Dots and in Situ Enzymatic Generation of Electron Donor. *Biosens. Bioelectron.* **2019**, *124–125*, 1–7. [CrossRef] [PubMed]
150. Wu, T.; Zhang, Y.; Wei, D.; Wang, X.; Yan, T.; Du, B.; Wei, Q. Label-Free Photoelectrochemical Immunosensor for Carcinoembryonic Antigen Detection Based on g-C_3N_4 Nanosheets Hybridized with Zn0.1Cd0.9S Nanocrystals. *Sens. Actuators B Chem.* **2018**, *256*, 812–819. [CrossRef]
151. Zhang, K.; Lv, S.; Zhou, Q.; Tang, D. CoOOH Nanosheets-Coated g-C_3N_4/$CuInS_2$ Nanohybrids for Photoelectrochemical Biosensor of Carcinoembryonic Antigen Coupling Hybridization Chain Reaction with Etching Reaction. *Sens. Actuators B Chem.* **2020**, *307*, 127631. [CrossRef]
152. Liu, X.P.; Chen, J.S.; Mao, C.J.; Jin, B.K. A Label-Free Photoelectrochemical Immunosensor for Carcinoembryonic Antigen Detection Based on a g-C_3N_4/CdSe Nanocomposite. *Analyst* **2021**, *146*, 146–155. [CrossRef]
153. Pang, X.; Cui, C.; Su, M.; Wang, Y.; Wei, Q.; Tan, W. Construction of Self-Powered Cytosensing Device Based on ZnO Nanodisks@g-C_3N_4 Quantum Dots and Application in the Detection of CCRF-CEM Cells. *Nano Energy* **2018**, *46*, 101–109. [CrossRef] [PubMed]
154. Peng, B.; Lu, Y.; Luo, J.; Zhang, Z.; Zhu, X.; Tang, L.; Wang, L.; Deng, Y.; Ouyang, X.; Tan, J.; et al. Visible Light-Activated Self-Powered Photoelectrochemical Aptasensor for Ultrasensitive Chloramphenicol Detection Based on DFT-Proved Z-Scheme Ag_2CrO_4/g-C_3N_4/Graphene Oxide. *J. Hazard. Mater.* **2021**, *401*, 123395. [CrossRef] [PubMed]
155. Li, F.; Yin, H.; Chen, Y.; Wang, S.; Li, J.; Zhang, Y.; Li, C.; Ai, S. Preparation of P-g-C_3N_4-WS_2 Nanocomposite and Its Application in Photoelectrochemical Detection of 5-Formylcytosine. *J. Colloid Interface Sci.* **2020**, *561*, 348–357. [CrossRef] [PubMed]
156. Yuan, C.; He, Z.; Chen, Q.; Wang, X.; Zhai, C.; Zhu, M. Selective and Efficacious Photoelectrochemical Detection of Ciprofloxacin Based on the Self-Assembly of 2D/2D g-C_3N_4/Ti_3C_2 Composites. *Appl. Surf. Sci.* **2021**, *539*, 148241. [CrossRef]
157. Cao, Y.; Wang, L.; Wang, C.; Hu, X.; Liu, Y.; Wang, G. Sensitive Detection of Glyphosate Based on a Cu-BTC MOF/g-C_3N_4 Nanosheet Photoelectrochemical Sensor. *Electrochim. Acta* **2019**, *317*, 341–347. [CrossRef]
158. Li, Z.; Dong, W.; Du, X.; Wen, G.; Fan, X. A Novel Photoelectrochemical Sensor Based on G-C_3N_4@CdS QDs for Sensitive Detection of Hg^{2+}. *Microchem. J.* **2020**, *152*, 104259. [CrossRef]
159. Cai, Z.; Rong, M.; Zhao, T.; Zhao, L.; Wang, Y.; Chen, X. Solar-Induced Photoelectrochemical Sensing for Dopamine Based on TiO_2 Nanoparticles on g-C_3N_4 Decorated Graphene Nanosheets. *J. Electroanal. Chem.* **2015**, *759*, 32–37. [CrossRef]
160. Liu, P.; Huo, X.; Tang, Y.; Xu, J.; Liu, X.; Wong, D.K.Y. A TiO_2 Nanosheet-g-C_3N_4 Composite Photoelectrochemical Enzyme Biosensor Excitable by Visible Irradiation. *Anal. Chim. Acta* **2017**, *984*, 86–95. [CrossRef] [PubMed]
161. Çakıroğlu, B.; Demirci, Y.C.; Gökgöz, E.; Özacar, M. A Photoelectrochemical Glucose and Lactose Biosensor Consisting of Gold Nanoparticles, MnO_2 and g-C_3N_4 Decorated TiO_2. *Sens. Actuators B Chem.* **2019**, *282*, 282–289. [CrossRef]
162. Zhang, X.Y.; Liu, S.G.; Zhang, W.J.; Wang, X.H.; Han, L.; Ling, Y.; Li, N.B.; Luo, H.Q. Photoelectrochemical Platform for Glucose Sensing Based on G-C_3N_4/$ZnIn_2S_4$ Composites Coupled with Bi-Enzyme Cascade Catalytic in-Situ Precipitation. *Sens. Actuators B Chem.* **2019**, *297*, 126818. [CrossRef]
163. Chen, D.; Jiang, D.; Du, X.; Zhou, L.; Huang, L.; Qian, J.; Liu, Q.; Hao, N.; Li, Y.; Wang, K. Engineering Efficient Charge Transfer Based on Ultrathin Graphite-like Carbon Nitride/WO_3 Semiconductor Nanoheterostructures for Fabrication of High-Performances Non-Enzymatic Photoelectrochemical Glucose Sensor. *Electrochim. Acta* **2016**, *215*, 305–312. [CrossRef]
164. Zhang, F.; Zhang, P.; Wu, Q.; Xiong, W.; Kang, Q.; Shen, D. Impedance Response of Photoelectrochemical Sensor and Size-Exclusion Filter and Catalytic Effects in $Mn_3(BTC)_2$/g-C_3N_4/TiO_2 Nanotubes. *Electrochim. Acta* **2017**, *247*, 80–88. [CrossRef]
165. Wang, Y.; Cheng, Y.; Wu, N.; Zhang, Z. Graphitic Carbon Nitride/Poly(3-Hexylthiophene) Nanocomposites for the Photoelectrochemical Detection of H_2O_2 in Living Cells. *ACS Appl. Nano Mater.* **2020**, *3*, 8598–8603. [CrossRef]
166. Wang, H.; Zhang, Q.; Yin, H.; Wang, M.; Jiang, W.; Ai, S. Photoelectrochemical Immunosensor for Methylated RNA Detection Based on G-C_3N_4/CdS Quantum Dots Heterojunction and Phos-Tag-Biotin. *Biosens. Bioelectron.* **2017**, *95*, 124–130. [CrossRef]
167. Wang, H.; Liu, P.; Jiang, W.; Li, X.; Yin, H.; Ai, S. Photoelectrochemical Immunosensing Platform for M. SssI Methyltransferase Activity Analysis and Inhibitor Screening Based on g-C_3N_4 and CdS Quantum Dots. *Sens. Actuators B Chem.* **2017**, *244*, 458–465. [CrossRef]
168. Li, X.; Yuan, Y.; Pan, X.; Zhang, L.; Gong, J. Boosted Photoelectrochemical Immunosensing of Metronidazole in Tablet Using Coral-like g-C_3N_4 Nanoarchitectures. *Biosens. Bioelectron.* **2019**, *123*, 7–13. [CrossRef]
169. Ouyang, X.; Tang, L.; Feng, C.; Peng, B.; Liu, Y.; Ren, X.; Zhu, X.; Tan, J.; Hu, X. Au/CeO_2/g-C_3N_4 Heterostructures: Designing a Self-Powered Aptasensor for Ultrasensitive Detection of Microcystin-LR by Density Functional Theory. *Biosens. Bioelectron.* **2020**, *164*, 112328. [CrossRef] [PubMed]
170. Wang, M.; Yin, H.; Zhou, Y.; Sui, C.; Wang, Y.; Meng, X.; Waterhouse, G.I.N.; Ai, S. Photoelectrochemical Biosensor for MicroRNA Detection Based on a MoS_2/g-C_3N_4/Black TiO_2 Heterojunction with Histostar@AuNPs for Signal Amplification. *Biosens. Bioelectron.* **2019**, *128*, 137–143. [CrossRef] [PubMed]
171. Dong, Y.X.; Cao, J.T.; Wang, B.; Ma, S.H.; Liu, Y.M. Exciton-Plasmon Interactions between CdS@g-C_3N_4 Heterojunction and Au@Ag Nanoparticles Coupled with DNAase-Triggered Signal Amplification: Toward Highly Sensitive Photoelectrochemical Bioanalysis of MicroRNA. *ACS Sustain. Chem. Eng.* **2017**, *5*, 10840–10848. [CrossRef]
172. Ma, Y.; Dong, Y.X.; Wang, B.; Ren, S.W.; Cao, J.T.; Liu, Y.M. CdS:Mn-Sensitized 2D/2D Heterostructured g-C_3N_4-MoS_2 with Excellent Photoelectrochemical Performance for Ultrasensitive Immunosensing Platform. *Talanta* **2020**, *207*, 120288. [CrossRef]

173. Dang, X.; Song, Z.; Zhao, H. Signal Amplified Photoelectrochemical Assay Based on Polypyrrole/g-C_3N_4/WO_3 Inverse Opal Photonic Crystals Triple Heterojunction Assembled through Sandwich-Type Recognition Model. *Sens. Actuators B Chem.* **2020**, *310*, 127888. [CrossRef]
174. Dang, X.; Zhang, X.; Zhao, H. Signal Amplified Photoelectrochemical Sensing Platform with G-C_3N_4/Inverse Opal Photonic Crystal WO_3 Heterojunction Electrode. *J. Electroanal. Chem.* **2019**, *840*, 101–108. [CrossRef]
175. Mak, W.C.; Beni, V.; Turner, A.P.F. Lateral-Flow Technology: From Visual to Instrumental. *TrAC-Trends Anal. Chem.* **2016**, *79*, 297–305. [CrossRef]
176. Zhu, H.; Fan, J.; Du, J.; Peng, X. Fluorescent Probes for Sensing and Imaging within Specific Cellular Organelles. *Acc. Chem. Res.* **2016**, *49*, 2115–2126. [CrossRef]
177. Tan, G.R.; Wang, M.; Hsu, C.Y.; Chen, N.; Zhang, Y. Small Upconverting Fluorescent Nanoparticles for Biosensing and Bioimaging. *Adv. Opt. Mater.* **2016**, *4*, 984–997. [CrossRef]
178. Han, J.; Burgess, K. Fluorescent Indicators for Intracellular PH. *Chem. Rev.* **2010**, *110*, 2709–2728. [CrossRef]
179. Wang, H.; Wang, D.; Wang, Q.; Li, X.; Schalley, C.A. Nickel(Ii) and Iron(Iii) Selective off-on-Type Fluorescence Probes Based on Perylene Tetracarboxylic Diimide. *Org. Biomol. Chem.* **2010**, *8*, 1017–1026. [CrossRef] [PubMed]
180. Kaczmarski, J.A.; Mitchell, J.A.; Spence, M.A.; Vongsouthi, V.; Jackson, C.J. Structural and Evolutionary Approaches to the Design and Optimization of Fluorescence-Based Small Molecule Biosensors. *Curr. Opin. Struct. Biol.* **2019**, *57*, 31–38. [CrossRef] [PubMed]
181. Nawrot, W.; Drzozga, K.; Baluta, S.; Cabaj, J.; Malecha, K. A Fluorescent Biosensors for Detection Vital Body Fluids' Agents. *Sensors* **2018**, *18*, 2357. [CrossRef] [PubMed]
182. Dodani, S.C.; He, Q.; Chang, C.J. A Turn-on Fluorescent Sensor for Detecting Nickel in Living Cells. *J. Am. Chem. Soc.* **2009**, *131*, 18020–18021. [CrossRef] [PubMed]
183. Bauch, M.; Toma, K.; Toma, M.; Zhang, Q.; Dostalek, J. Plasmon-enhanced fluorescence biosensors: A review. *Plasmonics* **2014**, *9*, 781–799. [CrossRef]
184. Serrano-Andrés, L.; Serrano-Pérez, J.J. Calculation of Excited States: Molecular Photophysics and Photochemistry on Display. In *Handbook of Computational Chemistry*; Springer: Berlin/Heidelberg, Germany, 2012; pp. 483–560. [CrossRef]
185. Girigoswami, K.; Akhtar, N. Nanobiosensors and Fluorescence Based Biosensors: An Overview. *Int. J. Nano Dimens.* **2019**, *10*, 1–17.
186. Tao, H.; Fan, Q.; Ma, T.; Liu, S.; Gysling, H.; Texter, J.; Guo, F.; Sun, Z. Two-Dimensional Materials for Energy Conversion and Storage. *Prog. Mater. Sci.* **2020**, *111*, 100637. [CrossRef]
187. Akada, K.; Terasawa, T.O.; Imamura, G.; Obata, S.; Saiki, K. Control of Work Function of Graphene by Plasma Assisted Nitrogen Doping. *Appl. Phys. Lett.* **2014**, *104*, 131602. [CrossRef]
188. Paquin, F.; Rivnay, J.; Salleo, A.; Stingelin, N.; Silva, C. Multi-Phase Semicrystalline Microstructures Drive Exciton Dissociation in Neat Plastic Semiconductors. *J. Mater. Chem. C* **2015**, *3*, 10715–10722. [CrossRef]
189. Lee, E.Z.; Jun, Y.S.; Hong, W.H.; Thomas, A.; Jin, M.M. Cubic Mesoporous Graphitic Carbon(IV) Nitride: An All-in-One Chemosensor for Selective Optical Sensing of Metal Ions. *Angew. Chemie-Int. Ed.* **2010**, *49*, 9706–9710. [CrossRef]
190. Kadam, A.N.; Moniruzzaman, M.; Lee, S.W. Dual Functional S-Doped g-C_3N_4 Pinhole Porous Nanosheets for Selective Fluorescence Sensing of Ag^+ and Visible-Light Photocatalysis of Dyes. *Molecules* **2019**, *24*, 450. [CrossRef] [PubMed]
191. Wang, S. g-C_3N_4 Nanosheets as "on-off-on" Selective Fluorescence Biosensor to Detect Ascorbic Acid via Redox Reaction. *J. Alloys Compd.* **2019**, *770*, 952–958. [CrossRef]
192. Obregón, S.; Vázquez, A.; Ruíz-Gómez, M.A.; Rodríguez-González, V. SBA-15 Assisted Preparation of Mesoporous g-C_3N_4 for Photocatalytic H_2 Production and Au^{3+} Fluorescence Sensing. *Appl. Surf. Sci.* **2019**, *488*, 205–212. [CrossRef]
193. Rong, M.; Lin, L.; Song, X.; Wang, Y.; Zhong, Y.; Yan, J.; Feng, Y.; Zeng, X.; Chen, X. Fluorescence Sensing of Chromium (VI) and Ascorbic Acid Using Graphitic Carbon Nitride Nanosheets as a Fluorescent "Switch". *Biosens. Bioelectron.* **2015**, *68*, 210–217. [CrossRef]
194. Shiravand, G.; Ghasemi, J.B.; Badiei, A.; Mohammadi Ziarani, G. A Dual-Emission Fluorescence Probe for Simultaneous Quantification of CN− and $Cr_2O_7^{2-}$ Ions Based on Modified g-C_3N_4. *J. Photochem. Photobiol. A Chem.* **2020**, *389*, 112261. [CrossRef]
195. Guo, X.; Wang, Y.; Wu, F.; Ni, Y.; Kokot, S. Preparation of Protonated, Two-Dimensional Graphitic Carbon Nitride Nanosheets by Exfoliation, and Their Application as a Fluorescent Probe for Trace Analysis of Copper(II). *Microchim. Acta* **2016**, *183*, 773–780. [CrossRef]
196. Salehnia, F.; Hosseini, M.; Ganjali, M.R. A Fluorometric Aptamer Based Assay for Cytochrome C Using Fluorescent Graphitic Carbon Nitride Nanosheets. *Microchim. Acta* **2017**, *184*, 2157–2163. [CrossRef]
197. Wang, S.; Lu, Q.; Yan, X.; Yang, M.; Ye, R.; Du, D.; Lin, Y. "On-Off-On" Fluorescence Sensor Based on g-C_3N_4 Nanosheets for Selective and Sequential Detection of Ag+ and S2-. *Talanta* **2017**, *168*, 168–173. [CrossRef]
198. Yang, C.; Wang, X.; Liu, H.; Ge, S.; Yan, M.; Yu, J.; Song, X. An Inner Filter Effect Fluorescent Sensor Based on G-C_3N_4 Nanosheets/Chromogenic Probe for Simple Detection of Glutathione. *Sens. Actuators B Chem.* **2017**, *248*, 639–645. [CrossRef]
199. Lv, J.; Feng, S.; Ding, Y.; Chen, C.; Zhang, Y.; Lei, W.; Hao, Q.; Chen, S.M. A High-Performance Fluorescent Probe for Dopamine Detection Based on g-C_3N_4 Nanofibers. *Spectrochim. Acta-Part A Mol. Biomol. Spectrosc.* **2019**, *212*, 300–307. [CrossRef]

200. Guo, X.; Huang, J.; Wang, M.; Wang, L. A Dual-Emission Water-Soluble g-C_3N_4@AuNCs-Based Fluorescent Probe for Label-Free and Sensitive Analysis of Trace Amounts of Ferrous (II) and Copper (II) Ions. *Sens. Actuators B Chem.* **2020**, *309*, 127766. [CrossRef]
201. Liu, H.; Wang, H.; Zhang, L.; Sang, Y.; Pu, F.; Ren, J.; Qu, X. Fe(III)-Oxidized Graphitic Carbon Nitride Nanosheets as a Sensitive Fluorescent Sensor for Detection and Imaging of Fluoride Ions. *Sens. Actuators B Chem.* **2020**, *321*, 128630. [CrossRef]
202. Bagheri, N.; Dastborhan, M.; Khataee, A.; Hassanzadeh, J.; Kobya, M. Synthesis of G-C_3N_4@CuMOFs Nanocomposite with Superior Peroxidase Mimetic Activity for the Fluorometric Measurement of Glucose. *Spectrochim. Acta-Part A Mol. Biomol. Spectrosc.* **2019**, *213*, 28–36. [CrossRef] [PubMed]
203. Zhang, X.L.; Zheng, C.; Guo, S.S.; Li, J.; Yang, H.H.; Chen, G. Turn-on Fluorescence Sensor for Intracellular Imaging of Glutathione Using g-C_3N_4 Nanosheet-MnO_2 Sandwich Nanocomposite. *Anal. Chem.* **2014**, *86*, 3426–3434. [CrossRef]
204. Guo, Z.; Li, B.; Zhang, Y.; Zhao, Q.; Zhao, J.; Li, L.; Feng, L.; Wang, M.; Meng, X.; Zuo, G. Acid-Treated Graphitic Carbon Nitride Nanosheets as Fluorescence Probe for Detection of Hemin. *ChemistrySelect* **2019**, *4*, 8178–8182. [CrossRef]
205. Guo, Z.; Zhao, Q.; Zhang, Y.; Li, B.; Li, L.; Feng, L.; Wang, M.; Meng, X.; Zuo, G. A Novel "Turn-on" Fluorescent Sensor for Hydrogen Peroxide Based on Oxidized Porous g-C_3N_4 Nanosheets. *J. Biomed. Mater. Res.-Part B Appl. Biomater.* **2020**, *108*, 1077–1084. [CrossRef]
206. Arabi, M.S.; Karami, C.; Taher, M.A.; Ahmadi, E. Fluorescence Detection of Laccases Activity by the Photoinduced Electron Transfer (PET) Process. *J. Biol. Inorg. Chem.* **2020**, *25*, 151–159. [CrossRef]
207. Hu, S.; Ouyang, W.; Guo, L.; Lin, Z.; Jiang, X.; Qiu, B.; Chen, G. Facile Synthesis of Fe_3O_4/g-C_3N_4/HKUST-1 Composites as a Novel Biosensor Platform for Ochratoxin A. *Biosens. Bioelectron.* **2017**, *92*, 718–723. [CrossRef]
208. Chan, M.H.; Liu, R.S.; Hsiao, M. Graphitic Carbon Nitride-Based Nanocomposites and Their Biological Applications: A Review. *Nanoscale* **2019**, *11*, 14993–15003. [CrossRef]
209. Yoo, S.M.; Jeon, Y.M.; Heo, S.Y. Electrochemiluminescence Systems for the Detection of Biomarkers: Strategical and Technological Advances. *Biosensors* **2022**, *12*, 738. [CrossRef]
210. Zheng, X.; Hua, X.; Qiao, X.; Xia, F.; Tian, D.; Zhou, C. Simple and Signal-off Electrochemiluminescence Immunosensor for Alpha Fetoprotein Based on Gold Nanoparticle-Modified Graphite-like Carbon Nitride Nanosheet Nanohybrids. *RSC Adv.* **2016**, *6*, 21308–21316. [CrossRef]
211. Zhang, M.; Chen, Z.; Qin, H.; Yang, X.; Cao, W.; Liu, S. G-C_3N_4-Heme Bound to Amyloid β Peptides: In-Situ Generation of the Secondary Co-Reactant for Dual-Enhanced Electrochemiluminescence Assay of Amyloid β Detection. *Electrochim. Acta* **2020**, *361*, 137096. [CrossRef]
212. Fang, J.; Zhao, G.; Dong, X.; Li, X.; Miao, J.; Wei, Q.; Cao, W. Ultrasensitive Electrochemiluminescence Immunosensor for the Detection of Amyloid-β Proteins Based on Resonance Energy Transfer between g-C_3N_4 and Pd NPs Coated NH2-MIL-53. *Biosens. Bioelectron.* **2019**, *142*, 111517. [CrossRef] [PubMed]
213. Wu, L.; Sha, Y.; Li, W.; Wang, S.; Guo, Z.; Zhou, J.; Su, X.; Jiang, X. One-Step Preparation of Disposable Multi-Functionalized g-C_3N_4 Based Electrochemiluminescence Immunosensor for the Detection of CA125. *Sens. Actuators B Chem.* **2016**, *226*, 62–68. [CrossRef]
214. Fan, Y.; Tan, X.; Ou, X.; Lu, Q.; Chen, S.; Wei, S. A Novel "on-off" Electrochemiluminescence Sensor for the Detection of Concanavalin A Based on Ag-Doped g-C_3N_4. *Electrochim. Acta* **2016**, *202*, 90–99. [CrossRef]
215. Liu, M.; Zhang, B.; Zhang, M.; Hu, X.; Chen, W.; Fang, G.; Wang, S. A Dual-Recognition Molecularly Imprinted Electrochemiluminescence Sensor Based on g-C_3N_4 Nanosheets Sensitized by Electrodeposited RGO-COOH for Sensitive and Selective Detection of Tyramine. *Sens. Actuators B Chem.* **2020**, *311*, 127901. [CrossRef]
216. Li, M.; Wang, C.; Liu, D. A Novel "off-on" Electrochemiluminescence Sensor Based on Highly Efficient Resonance Energy Transfer in C-g-C_3N_4/CuO Nanocomposite. *Anal. Chim. Acta* **2020**, *1138*, 30–37. [CrossRef]
217. Fu, X.; Feng, J.; Tan, X.; Lu, Q.; Yuan, R.; Chen, S. Electrochemiluminescence Sensor for Dopamine with a Dual Molecular Recognition Strategy Based on Graphite-like Carbon Nitride Nanosheets/3,4,9,10-Perylenetetracarboxylic Acid Hybrids. *RSC Adv.* **2015**, *5*, 42698–42704. [CrossRef]
218. Lu, Q.; Zhang, J.; Liu, X.; Wu, Y.; Yuan, R.; Chen, S. Enhanced Electrochemiluminescence Sensor for Detecting Dopamine Based on Gold Nanoflower@graphitic Carbon Nitride Polymer Nanosheet-Polyaniline Hybrids. *Analyst* **2014**, *139*, 6556–6562. [CrossRef]
219. Zhou, C.; Chen, Y.; Shang, P.; Chi, Y. Strong Electrochemiluminescent Interactions between Carbon Nitride Nanosheet-Reduced Graphene Oxide Nanohybrids and Folic Acid, and Ultrasensitive Sensing for Folic Acid. *Analyst* **2016**, *141*, 3379–3388. [CrossRef]
220. Yin, J.; Chen, X.; Chen, Z. Quenched Electrochemiluminescence Sensor of ZnO@g-C_3N_4 Modified Glassy Carbon Electrode for Fipronil Determination. *Microchem. J.* **2019**, *145*, 295–300. [CrossRef]
221. Fan, Z.; Lin, Z.; Wang, Z.; Wang, J.; Xie, M.; Zhao, J.; Zhang, K.; Huang, W. Dual-Wavelength Electrochemiluminescence Ratiometric Biosensor for NF-KB P50 Detection with Dimethylthiodiaminoterephthalate Fluorophore and Self-Assembled DNA Tetrahedron Nanostructures Probe. *ACS Appl. Mater. Interfaces* **2020**, *12*, 11409–11418. [CrossRef] [PubMed]
222. Wang, Y.Z.; Hao, N.; Feng, Q.M.; Shi, H.W.; Xu, J.J.; Chen, H.Y. A Ratiometric Electrochemiluminescence Detection for Cancer Cells Using G-C_3N_4 Nanosheets and Ag-PAMAM-Luminol Nanocomposites. *Biosens. Bioelectron.* **2016**, *77*, 76–82. [CrossRef] [PubMed]
223. Ma, H.; Liu, Y.; Zhao, Y.; Li, L.; Zhang, Y.; Wu, D.; Wei, Q. Ultrasensitive Immunoassay of Insulin Based on Highly Efficient Electrochemiluminescence Quenching of Carboxyl-Functionalized g-C_3N_4 through Coreactant Dual-Consumption by NiPd-DNAzyme. *J. Electroanal. Chem.* **2018**, *818*, 168–175. [CrossRef]

224. Zhou, M.; Pu, Y.; Wu, Q.; Wang, P.; Liu, T.; Zhang, M. 2D Hexagonal SnS_2 Nanoplates as Novel Co-Reaction Accelerator for Construction of Ultrasensitive g-C_3N_4-Based Electrochemiluminescent Biosensor. *Sens. Actuators B Chem.* **2020**, *319*, 128298. [CrossRef]
225. Shao, H.; Lin, H.; Lu, J.; Hu, Y.; Wang, S.; Huang, Y.; Guo, Z. Potential-Resolved Faraday Cage-Type Electrochemiluminescence Biosensor for Simultaneous Determination of MiRNAs Using Functionalized g-C_3N_4 and Metal Organic Framework Nanosheets. *Biosens. Bioelectron.* **2018**, *118*, 247–252. [CrossRef]
226. Li, L.; Zhao, Y.; Li, X.; Ma, H.; Wei, Q. Label-Free Electrochemiluminescence Immunosensor Based on Ce-MOF@g-C_3N_4/Au Nanocomposite for Detection of N-Terminal pro-B-Type Natriuretic Peptide. *J. Electroanal. Chem.* **2019**, *847*, 113222. [CrossRef]
227. Xu, H.; Zhu, X.; Dong, Y.; Wu, H.; Chen, Y.; Chi, Y. Highly Sensitive Electrochemiluminescent Sensing Platform Based on Graphite Carbon Nitride Nanosheets for Detection of Pyrophosphate Ion in the Synovial Fluid. *Sens. Actuators B Chem.* **2016**, *236*, 8–15. [CrossRef]
228. Wu, L.; Hu, Y.; Sha, Y.; Li, W.; Yan, T.; Wang, S.; Li, X.; Guo, Z.; Zhou, J.; Su, X. An "in-Electrode"-Type Immunosensing Strategy for the Detection of Squamous Cell Carcinoma Antigen Based on Electrochemiluminescent AuNPs/g-C_3N_4 Nanocomposites. *Talanta* **2016**, *160*, 247–255. [CrossRef]
229. Liu, X.; Wang, Q.; Chen, J.; Chen, X.; Yang, W. Ultrasensitive Electrochemiluminescence Biosensor for the Detection of Tumor Exosomes Based on Peptide Recognition and Luminol-AuNPs@g-C_3N_4 Nanoprobe Signal Amplification. *Talanta* **2021**, *221*, 121379. [CrossRef]
230. Liu, J.L.; Jiang, J.; Zhang, J.Q.; Chai, Y.Q.; Xiao, Q.; Yuan, R. The Combination of Ternary Electrochemiluminescence System of G-C_3N_4 Nanosheet/TEA/Cu@Cu_2O and G-Quadruplex-Driven Regeneration Strategy for Ultrasensitive Bioanalysis. *Biosens. Bioelectron.* **2020**, *152*, 112006. [CrossRef] [PubMed]
231. Cheng, J.L.; Liu, X.P.; Chen, J.S.; Mao, C.J.; Jin, B.K. Highly Sensitive Electrochemiluminescence Biosensor for VEGF165 Detection Based on a G-C_3N_4/PDDA/CdSe Nanocomposite. *Anal. Bioanal. Chem.* **2020**, *412*, 3073–3081. [CrossRef] [PubMed]